

https://dspace.org/

A Review of the Stope Support System at Impala Bafokeng North Shaft Owing to Stope Closure at Shallow Mining Depths

Walsh, Trevor

2024

University of the Witwatersrand, Johannesburg

https://hdl.handle.net/10539/45910

Walsh, Trevor. (2024). A Review of the Stope Support System at Impala Bafokeng North Shaft Owing to Stope Closure at Shallow Mining Depths [Master`s dissertation, University of the Witwatersrand, Johannesburg]. WIReDSpace.

Downloaded from a DSpace repository. https://dspace.org/

School of Mining Engineering



UNIVERSITY OF THE
WITWATERSRAND,
JOHANNESBURG

A REVIEW OF THE STOPE SUPPORT SYSTEM AT IMPALA BAFOKENG NORTH SHAFT OWING TO STOPE CLOSURE AT SHALLOW MINING DEPTHS

Trevor Walsh

1250007

Supervisor: Professor T Stacey

A research report submitted to the Faculty of Engineering and the Built Environment, University of the Witwatersrand, Johannesburg, in partial fulfillment of the requirements for the degree of Master of Science

Johannesburg, 2024

DECLARATION

I declare that this report is my own, unaided work. I have read the University Policy on Plagiarism and hereby confirm that no plagiarism exists in this report. I also confirm that there is no copying nor is there any copyright infringement. I willingly submit to any investigation in this regard by the School of Mining Engineering and I undertake to abide by the decision of any such investigation.



Signature of Candidate

29/04/2024

Date

ABSTRACT

Impala Bafokeng's North Shaft is a shallow platinum mine on the western limb of the Bushveld Igneous Complex. Shallow mines experience very little horizontal stress which leads to a support issue of the tensile zone. North Shaft relies heavily on mine pole support due to the requirements for a stiff support system. Elongate support failure in the deeper parts of the mine have occurred due to a change in the loading environment. The support failure has resulted in inadequate support resistance in the back areas and some large falls of ground.

In this research report the Hybrid Section stope closure rate was measured. The closure does not appear to be linked to a detachment of a hangingwall parting. The ground penetrating radar scans and borehole data correlate with the observations. The falls of ground are structure related and occur in the back areas of the panel after the elongate support had failed.

The footwall material is weaker than the hangingwall material and the pillar punches into the footwall. The footwall fractures and tensile cracks in the panel footwall indicate that the stresses are forced to move horizontally due to the footwall 4 parting plane. The footwall thrusts into the panel causing the high closure observed. The combination of a shorter panel length and pencil sticks would provide adequate support for the high closure rates observed.

ACKNOWLEDGMENTS

This research was made possible by Impala Bafokeng, the contributions made by the company in terms of monitoring equipment and study assistance have been invaluable. Thanks to Professor Thomas Stacey who supervised the research and provided feedback and support. Thanks to my colleagues Nelson Mandhaze and Lawrence Phale for assistance with data collection. A huge thank you to my wife Joanne Walsh for her unwavering support throughout the years.

TABLE OF CONTENTS

DECLARATION ii

ABSTRACT iii

ACKNOWLEDGMENTS iv

LIST OF FIGURES vii

LIST OF TABLES x

LIST OF ABBREVIATIONS AND SYMBOLS xi

1 INTRODUCTION 1

1.1 Locality 2

1.2 Mine Background 2

1.3 Problem Statement 3

1.4 Justification for Research 4

1.5 Research Objectives 5

1.6 Support Design Background 5

1.7 Pillar Background 9

1.8 Monitoring Systems 12

2 LITERATURE REVIEW 13

2.1 Introduction 13

2.2 Panel Span Design 13

2.3 Support Design Methodology 14

2.4 Tensile Zone 14

2.5 Key Concepts, Theories and Studies 16

2.6 Key Debates 22

3 RESEARCH METHODOLOGY 33

3.1 Closure Logger Studies 33

3.2 Research Design 33
3.3 Borehole Camera Observations 35
3.4 Ground Penetrating Radar 36
3.5 Visual Observations 38
4 RESULTS AND DISCUSSION 39
4.1 Data Collection Process 39
4.2 Data Validation Process for Closure Loggers 45
4.3 Data Analysis Approach 46
4.4 Changes to Support Strategy 48
4.5 Unturned Mine Poles Versus Pencil Sticks 49
4.6 Pencil Stick Monitoring 51
4.7 Short Panel Observations 52
4.8 Footwall Heave Hypothesis 53
5 CONCLUSIONS AND RECOMMENDATIONS 55
5.1 Introduction 55
5.2 Research Observations 55
5.3 Research Limitations 56
5.4 Recommendations 57
5.5 Recommendations For Future Research Work 57
6 REFERENCE LIST 58

LIST OF FIGURES

Figure 1.1: Location of the mine within the Bushveld Igneous Complex 2
Figure 1.2: Plan view of North Shaft. 3
Figure 1.3: Plan view of Merensky Section on Microstation. 4
Figure 1.4: Failed mine poles in the back area of stopes. 5
Figure 1.5: Tributary Area illustration. 6
Figure 1.6: Mine poles 6
Figure 1.7: Support standard for a Merensky Reef stope. 7
Figure 1.8: Telescopic drill rig and stabilizer. 8
Figure 1.9: In-stope resin bolt over the face. 8
Figure 1.10: Conventional Section mining layout with satellite pillars. 9
Figure 1.11: Hybrid Section mining layout. 10
Figure 1.12: Vertical pillar stress through different regions of the pillar. 11
Figure 1.13: Bracket pillars along prominent regional geological structures. 11
Figure 1.14: Rocktale monitoring device. 12
Figure 2.1: The engineering circle of design 14
Figure 2.2: Variation in mining environments with depth 15
Figure 2.3: Tensile zone above shallow stopes at various depths 16
Figure 2.4: Regional pillar and bracket pillar. 17
Figure 2.5: Tributary Area Theory demonstration of load attributed to each pillar 17
Figure 2.6: Flow chart for crush pillar design 18
Figure 2.7: Pillar residual strength as a function of w/h ratio. 18
Figure 2.8: Comparison of the formula and measurements of peak pillar strength 19
Figure 2.9: Probability density function sectioned according to performance specification 20
Figure 2.10: Closure logger installed in a stope panel. 21
Figure 2.11: Historic closure measurements conducted on the Mine 22
Figure 2.12: Stratigraphic column of the BRPM mining locality 23
Figure 2.13: Wedge failure between joint sets. 24
Figure 2.14: New modified stability graph plot of stopes supported on mine poles with a support resistance of 128 kN/m^2 25

Figure 2.15: Calculated convergence rates based on closure loggers installation position. 27
Figure 2.16: Manual closure measurement tool 27
Figure 2.17: Continuous closure measurement and typical terms used 28
Figure 2.18: A cross section of a drive showing deformation that has taken place 29
Figure 2.19: GPR scans and borehole camera correlation on pillar 30
Figure 2.20: Design chart for crush pillars 32
Figure 3.1: Location of closure loggers installed on 5 and 6 levels. 33
Figure 3.2: Closure logger installation by the author. 34
Figure 3.3: Closure Logger installations plotted on plan. 35
Figure 3.4: Rock Engineering Department borehole camera. 35
Figure 3.5: Instrumentation locations for the initial study. 36
Figure 3.6: Simplified system block diagram of a GPR system 37
Figure 3.7: Sub Surface Profiler used for GPR analysis 37
Figure 3.8: Crush pillar scaling at N15 Level. 38
Figure 4.1: FOG along C-packs prevented further unravelling. 39
Figure 4.2: Breakdown of FOG's from 2019 - 2023 by geological discontinuity. 40
Figure 4.3: Screenshot taken from borehole camera investigations. 41
Figure 4.4: Pillar observed during underground investigations. 42
Figure 4.5: Location of pillar observed. 42
Figure 4.6: Hangingwall condition around the crush pillar. 43
Figure 4.7: Footwall fracturing and heave around a crush pillar footwall. 43
Figure 4.8: Tensile cracks in the footwall. 44
Figure 4.9: The author conducting GPR scans along the Roadway. 44
Figure 4.10: Closure logger data after 5 weeks (Unit 3131). 45
Figure 4.11: Closure logger data after 8 weeks (Unit 3134). 45
Figure 4.12: Closure Logger data after 5 months (Unit 3131) 46
Figure 4.13: GPR scan of 14 Level Roadway. 47
Figure 4.14: Contact from Merensky hangingwall to Norite. 47
Figure 4.15: GPR scan of 15 Level north 02 raise line. 48
Figure 4.16: Load-deformation chart of C-Pack. 48
Figure 4.17: C-pack construction and testing at the CSIR Laboratory in Johannesburg. 49

Figure 4.18: Load-deformation chart of various size mine poles. 50
Figure 4.19: Pencil sticks selected for load deformation testing. 50
Figure 4.20: Load-deformation chart of 18 cm pencil sticks, 140 mm length. 51
Figure 4.21: N15LN02 Panel 001E layout on Microstation. 52
Figure 4.22: Pencil sticks showing rapid yielding. 52
Figure 4.23: Panel 006W layout on Microstation. 53
Figure 4.24: Mine pole support in short panel. 53
Figure 5.1: Illustration of stress transfer into footwall. 56
Figure 5.2: Illustration of footwall failure and heave into the panel. 56

LIST OF TABLES

Table 4.1: Load capacities of mine poles 49
Table 4.2: FW4 shear depth from exploration drilling 54

LIST OF ABBREVIATIONS AND SYMBOLS

Abbreviation	Description
PGM	Platinum Group Metal
UG2	Upper Group Two Reef
GPR	Ground Penetrating Radar
SSP	Sub Surface Profiler
APS	Average Pillar Stress
ASG	Advanced Strike Gully
TAT	Tributary Area Theory
TARP	Trigger Action Response Plan
LHD	Load, Haul, Dump Loader
BIC	Bushveld Igneous Complex
FOG	Fall of Ground
LiDar	Light Detection and Ranging
RMR	Rock Mass Rating
UCS	Unconfined Compressive Strength

Symbol	Description	Units
k	Rockmass unit strength	MPa
w_e	Effective width	m
h_e	Effective height	m
h	Height	m
w	Width	m

1 INTRODUCTION

The Bushveld Igneous Complex (BIC) is a layered igneous intrusion that is mined for Platinum Group Minerals (PGM's). Much of the mining takes place using conventional mining methods. Shallow mines experience very little horizontal stress which leads to a support issue of the tensile zone. When the tensile zone interacts with low angled geological structures, it can lead to instability. North Shaft's support designs have historically been of an empirical nature and progressive improvements to the support design have taken place over the years. The mine relies heavily on elongate support due to the requirements for a stiff support system to prevent any unravelling from taking place.

A recent occurrence of elongate support failure in the deeper parts of the mine raised concerns about the suitability of the support design for the loading environment. High closure rates were observed and this has led to the early stoppage of panels and reduced extraction on the mine. The support failure caused there to be inadequate support resistance in the back areas which resulted in large falls of ground in the back areas of some panels.

The report will give a background on the current support design, research into the cause of the problem and potential solutions. Section 1 of the report consists of an introduction to the mine, problem statement and background on the support design and pillars used. Section 2 includes a literature review of rock engineering design processes, pillar design, elongate support performance and closure measurement, followed by a brief introduction of key concepts, theories and studies. Case studies of neighbouring mines were also considered. In Section 3, the research methodology and sources of data utilised are discussed. Section 4 includes the data validation and analysis. Results and discussions of instrumentation and visual observations. This includes results of new support items that were tested. Section 5 includes the conclusions drawn from this study and recommendations as well as recommendations for future work.

1.1 Locality

The BIC spans approximately 350 km from east to west and has three major outcrops, the northern, eastern and western limbs. Impala Bafokeng's North Shaft is situated within the western limb of the BIC between the Pilanesberg and Rustenburg (Figure 1.1). The mine is approximately 30 km north of Rustenburg, in the North-West Province. The PGM's mined are the Merensky reef, mining of which was established first and the UG2 reef mining was established second.

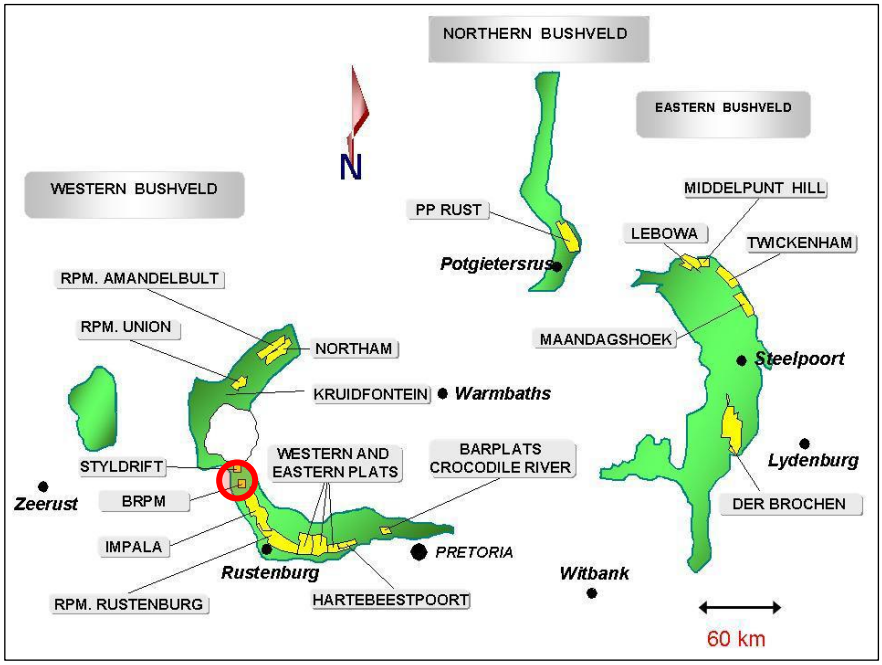

Figure 1.1: Location of the mine within the Bushveld Igneous Complex (Watson, et al., 2010).

1.2 Mine Background

Impala Bafokeng consists of two conventionally mined workings that are accessed by decline systems, namely North and South Shafts. Styldrift is the vertical Shaft, which is mechanised and is located approximately 5 km to the north of the two conventional shafts. North Shaft is a shallow tabular hard-rock mine that exploits the Merensky and UG2 reef horizons. A mix of conventional scattered breast mining and hybrid mining takes place. The UG2 reef is currently being mined in the shallower portions of the mine between 100 m and 350 m depth. A reef middling of approximately 70 m is consistent across the workings. The Merensky reef is currently being mined between 400 m and 600 m depth. The shaft bottom is

approximately 670 m below surface and the mine is therefore considered a shallow working environment.

The Hybrid Section consists of mechanised on reef development with conventional scattered breast stoping and is located at the deepest workings of the mine (Figure 1.2). Ore is transported along raise lines using a winch, into a muckbay. A load, haul, dump loader (LHD) is then used to transport the ore to the strike conveyor belts. The strategy for the Hybrid Section was to develop on-reef to reduce capital expenditure and time to access reef.

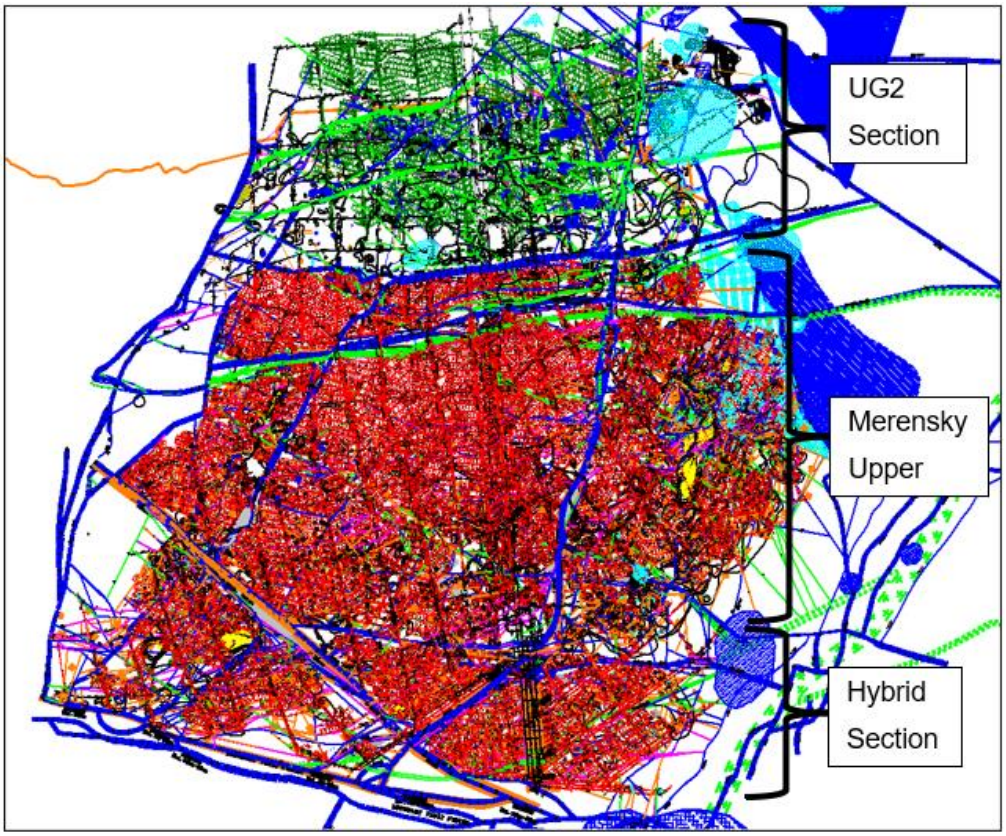

Figure 1.2: Plan view of North Shaft.

1.3 Problem Statement

Shallow mining depths have meant that North Shaft stopes have previously experienced very low closure rates. The first raise line that was established and mined at 15 level (Figure 1.3), experienced higher than expected closure rates which led to the failure of mine pole support units. Early stoppages occurred in some panels and sweepings were lost. The safety risk and the loss of reserves

necessitated a review of the stope support system. The mine needed to ensure a safe mining environment for the workforce and the optimum extraction of the mineral reserves.

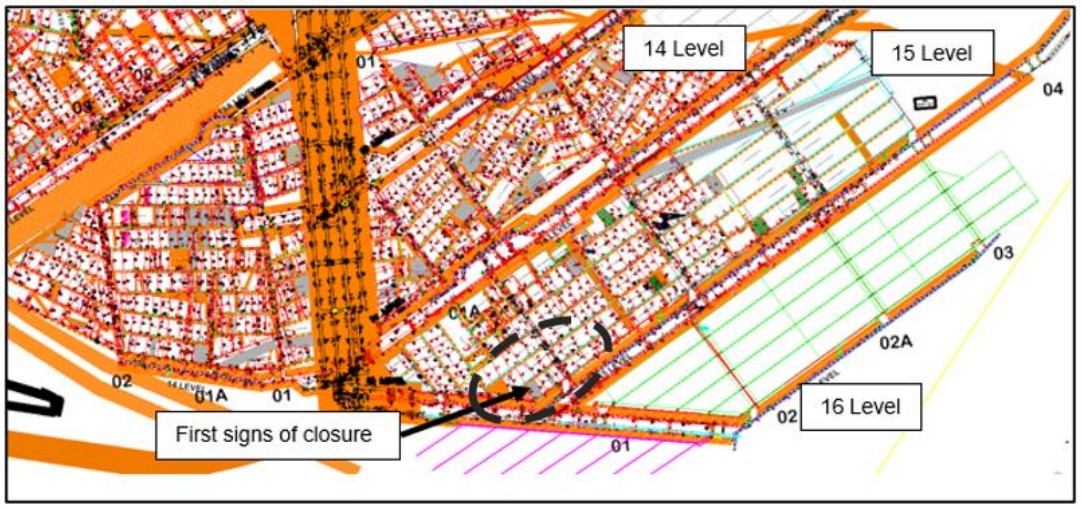

Figure 1.3: Plan view of Merensky Section on Microstation.

1.4 Justification for Research

The stope panel support system at North Shaft is designed to carry the deadweight up to the tensile zone. At shallow mining depth, little to no closure is expected (Jager & Ryder, 1999). The support system is designed to be stiff and active. The design is consistent with shallow mining support requirements of depths of less than 1000 m. The mine pole support was found to be splitting and buckling in the back areas of the panel from as little as 20 m away from the face (Figure 1.4). This led to the finding that the closure rate had increased rapidly from previously mined stopes. This study was aimed at adapting the support design for the new conditions encountered.



Figure 1.4: Failed mine poles in the back area of stopes.

1.5 Research Objectives

The main objectives of the study are to:

- Fully understand the rate of closure and its effects on the support system in use; and
- Adapt the support design to cater for the conditions encountered.

The expected benefits of the study include improved safety in the workplace. An appropriate support system would reduce stoppages and redevelopment of panels. The financial benefits include reduced loss of ground to pillars which are required to stabilize the stopes. The revenue obtained from being able to sweep all the panels up to the face area would benefit the mine.

1.6 Support Design Background

The support design is based on tributary area theory (TAT). The theory refers to the area surrounding a support unit that each individual support unit caters for (Figure 1.5). The distances between support units (A and B) are divided between the adjacent units to determine the total area that the unit (C) will need to support.

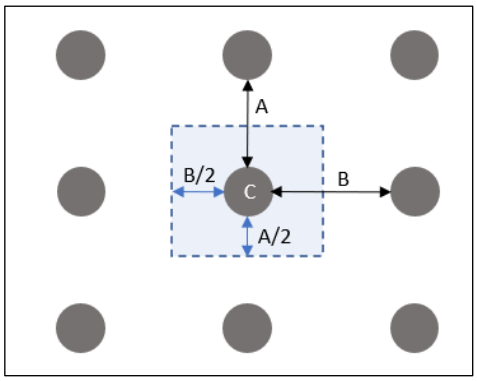

Figure 1.5: Tributary Area illustration.

The support design of North Shaft relies heavily on mine poles. A mine pole refers to an unturned elongate; mine poles are generally grown from a eucalyptus tree (Figure 1.6). The width of the mine pole is measured diametrically across the end of the pole. The mine poles are cheap compared to hydraulic props. The mine poles are readily available and simple to install. At shallow depth, mines generally have a low dynamic support requirement which makes the mine pole a suitable choice due to its stiff nature. The mine poles are installed in combination with a pre-stressing device. The mine pole becomes an active support unit which is ideal for mining at shallow depths.



Figure 1.6: Mine poles (Khosa, 2022).

The mine support standard includes temporary support in the form of mechanical props and safety nets during the day shift. Mine poles are required to support the geological structures and prevent keyblock failure in the face area. The face area is generally accepted as 0 m to 12 m up to the last line of sweepings. The back area support consists of ‘breaker lines’, clusters of three mine poles (Figure 1.7).

The clusters are installed to support the tensile zone which will be expanded on further in this report.

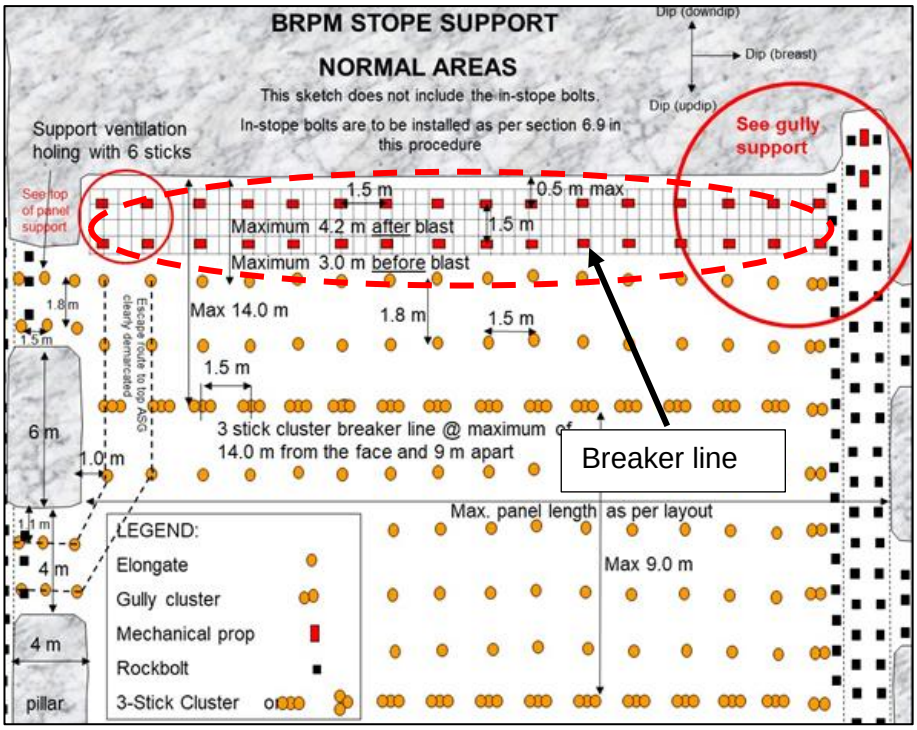

Figure 1.7: Support standard for a Merensky Reef stope.

1.6.1 In-stope Bolt Support

In-stope bolts are utilised that are 1.2 m in length. The bolts are 16 mm Secura Bolts and are installed with resin. A specially designed, telescopic drill rig with a stinger was utilized. The stinger assists with stabilizing the rig to reduce risk to the rock drill operator whilst drilling (Figure 1.8).



Figure 1.8: Telescopic drill rig and stabilizer.

The low stope width of 1.2 - 1.3 m meant that a 1.2 m bolt was challenging to fit. The low stope width would require that the bolts be coupling bolts to fit within the low working height. Coupling bolts, however, have several disadvantages which include higher costs. Larger drill holes are required for the coupler and there is a high risk of poor installation. The alternative strategy employed was to install the bolts at an angle of 60 - 70° over the face. The bolts were then able to fit as a single piece of steel. A benefit of the design was that the rockbolts provide support in the otherwise unsupported face area after the blast. The bolts needed to be drilled close to the face to take advantage of this aspect (Figure 1.9).

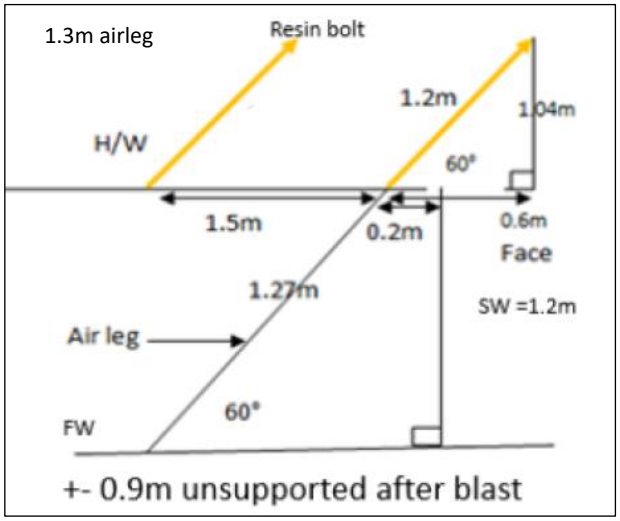

Figure 1.9: In-stope resin bolt over the face.

The effective installation height of the bolts did not exceed the fallout thickness. The bolts are therefore not considered further in this report beyond their ability to support keyblocks and assist with beam building which is still an important aspect. The drawback to this support strategy is that the support thickness is reduced. The angle of installation reduced the rockbolts effective support height to approximately 1 m.

1.7 Pillar Background

The Upper Section of the mine makes use of a yield pillar design between the panels, pillars 6 m long and 4 m wide were employed. The Upper Section of the mine is fully conventional and was designed with scattered satellite regional pillars. The pillars increase in size with depth, they are approximately 25 m wide and 25 m long (Figure 1.10). The satellite pillars provide flexibility to the stoping as they can be moved locally to areas of geolosses created by potholes or poor ground.

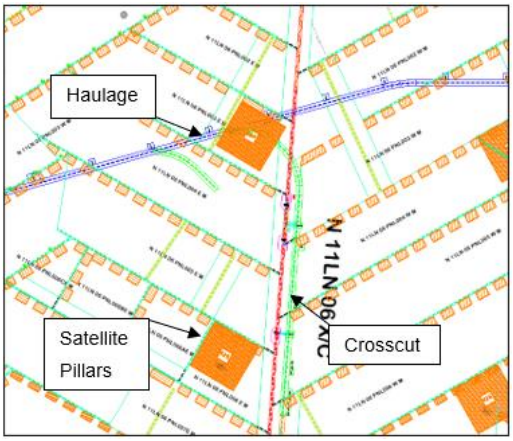

Figure 1.10: Conventional Section mining layout with satellite pillars.

The Hybrid Section is serviced with on-reef mechanised roadways that need to remain stable over the life of the mine. Strike stability pillars with a minimum width of 12 m were designed on either side of the roadways and belts (Figure 1.11). The Hybrid Section's in-stope pillars were designed to crush, they are 6 m long and 3 m wide.

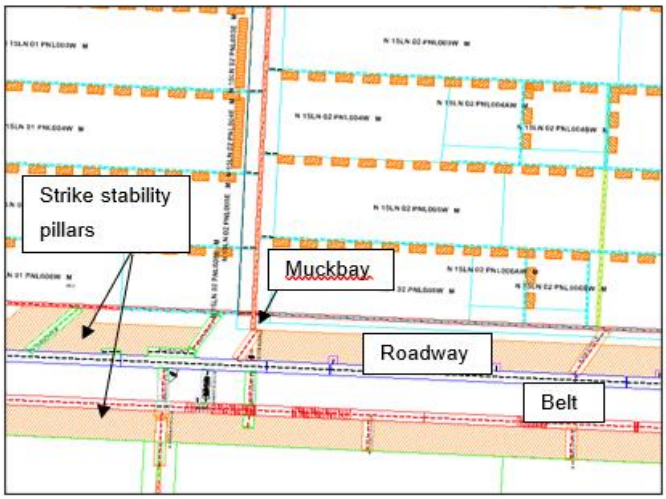

Figure 1.11: Hybrid Section mining layout.

The Hedley and Grant pillar strength formula (Ozbay, et al., 1995) in Equation 1.1 was used for the pillar design, where *k* is the rockmass unit strength, commonly 2/3 of the unconfined compressive strength (UCS) of a core sample. An alternative is the UCS x the Rock Mass Rating (RMR) of the rockmass. The *w* is the effective width of the pillar and *h* is the effective height.

$$Pillar\ Strength = \mathrm{k}\frac{w^{0.5}}{h^{0.75}}$$ ***Equation 1.1***

The pillars were modelled (Figure 1.12) using Flac3D by MLB Consulting (Le Bron, 2015a), and the average pillar stress (APS) was calculated and then compared with the tributary area theory (TAT). The corners of the pillars were predicted to experience higher strains than the core of the crush pillars. Slabbing along the sides of the pillars was predicted which led to a recommendation to pin the sidewalls along the gullies. A k-value of 58 MPa was calculated based on back analysis of pillars at the Hybrid Section (Le Bron, 2015b).

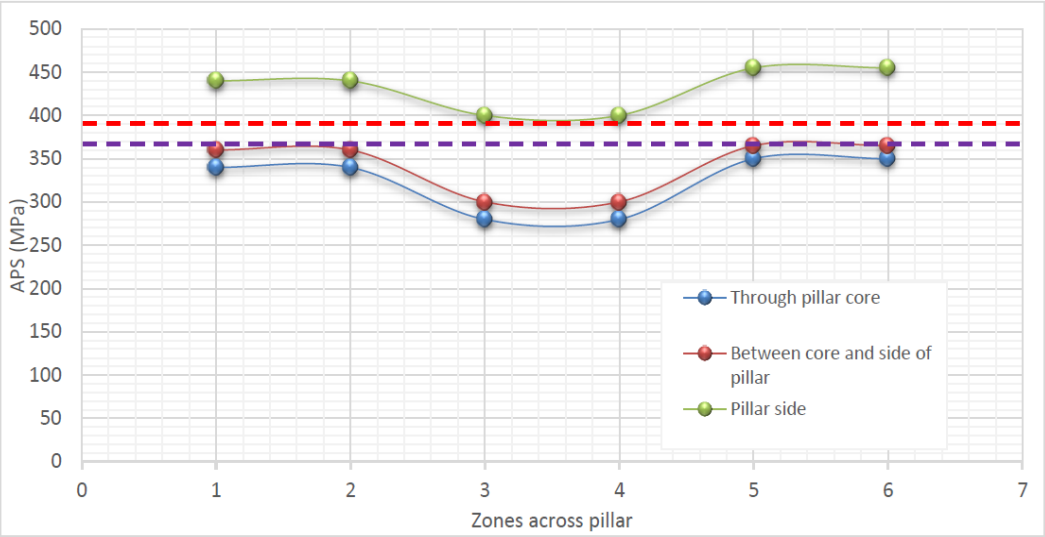

Figure 1.12: Vertical pillar stress through different regions of the pillar. Red is APS based on TAT, and purple is APS based on FLAC3D (Le Bron, 2015a).

Additional pillars are left as bracket pillars along prominent geological structures such as the 'South Shaft Shear Zone' and the 'Walsh Fault'. The shear zone is a zone of very poor rock mass approximately 20 m wide with a displacement of up to 25 m. The Walsh Fault displaces approximately 15 m and has a very poor rock mass quality around it (Figure 1.13). A large pillar was left over the Hybrid Section declines to protect the access way from any stress interaction.

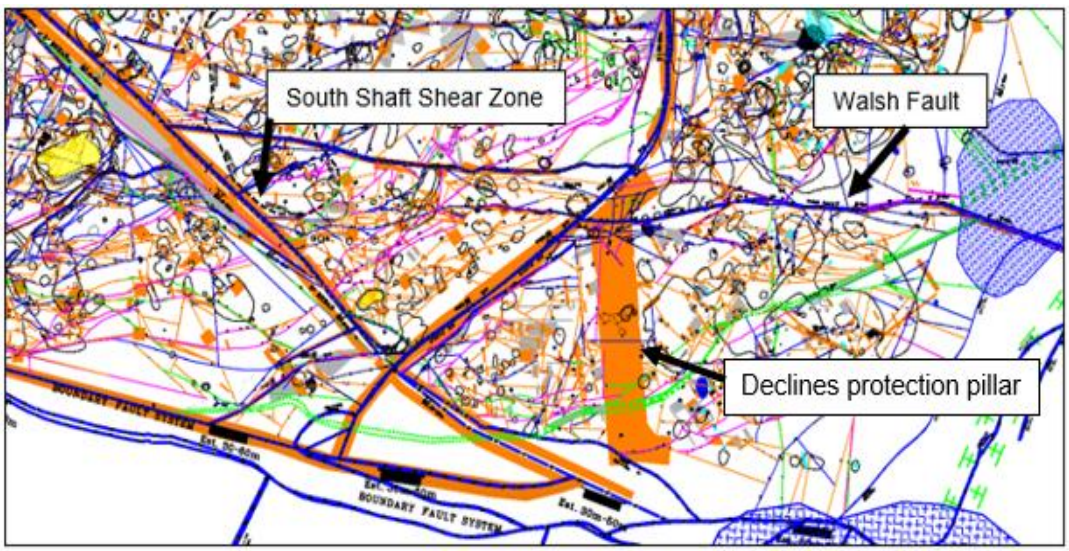

Figure 1.13: Bracket pillars along prominent regional geological structures.

1.8 Monitoring Systems

The widespread support failure of elongates had not been experienced before the current 15 level stopes had been mined. Mining on 14 level showed no signs of support failure even though the mining was only 30 m shallower. The support design had proven itself historically to be robust and capable of supporting the fallout height. Rocktale early warning devices have been used as safety warning devices in gullies of panels up to a height of 2.7 m (Figure 1.14). The Rocktale is a mechanical warning device. Lights and reflective tape are triggered if there is any separation between the head unit and the pins along the pipe.

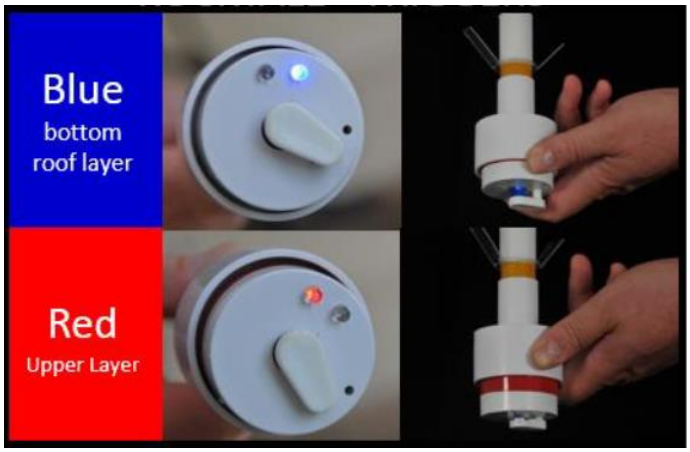

Figure 1.14: Rocktale monitoring device.

2 LITERATURE REVIEW

2.1 Introduction

Very few mines are using a proper engineering approach to stope panel and support design (Swart & Handley, 2004). Instability is linked to failure along geological structures but the mines do not make use of any design methodology based on structural analysis (Swart & Handley, 2004).

There is a huge number of variables within the support design and the implementation process. The key to improving rock engineering designs is to reduce the uncertainties around the geotechnical conditions. They include block size, loading rate, geological discontinuities, rock mass strength, shear strength and discontinuity spacing. The variables around implementation include variations in installation quality, adherence to patterns and spacing and not identifying a change in ground conditions (Dunn, 2013).

2.2 Panel Span Design

The cause of stope panel collapses in shallow mines is often linked to excessive panel lengths. The length is chosen according to what worked in the past and based on rockmass rating systems. A critical panel span design chart was empirically developed however the rating system was not comprehensive (York, et al., 1998).

A design methodology was developed for stable stope spans. The method involved the combination of empirical, analytical and observational design methods. Analytical design methods such as numerical design and structural analysis can compare the stope panel stability with varying input parameters. Some of the methodologies include keyblock or wedge type analysis, numerical stress analysis and beam-type analysis. Observational design methods include the monitoring of ground movement during mining (Swart & Handley, 2004).

2.3 Support Design Methodology

A simple guideline was developed with six design principles for rock engineering design (Bieniawski, 1992). Stacey (2009) added to this body of work by suggesting a difference between defining and executing a design. He developed a 10-step design process (Figure 2.1). The circle of design reflects the emphasis placed on review and monitoring. Both authors aimed to reduce uncertainty and add focus on monitoring and optimisation.

The support design methodology can be applied for the support units chosen to cater for the high closure rates in the hybrid section.

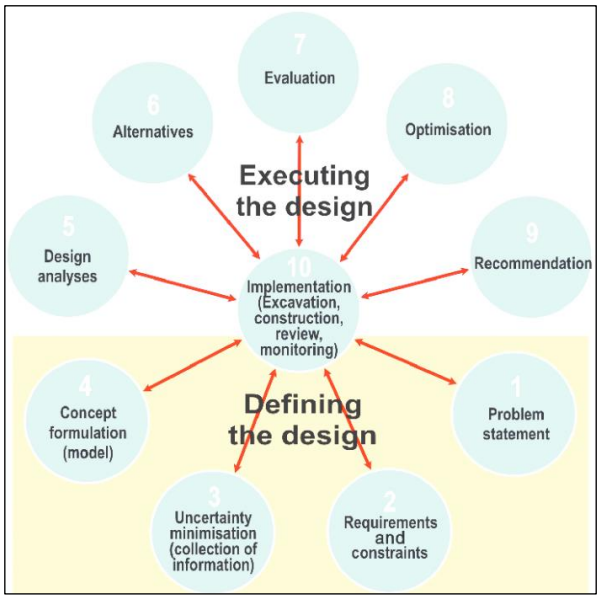

Figure 2.1: The engineering circle of design (Stacey, 2009).

2.4 Tensile Zone

Shallow mines experience difficulties with the 'tensile zone' in the hangingwall. The tensile zone is the area directly above the stope where horizontal clamping forces are close to zero. The tensile zone is especially important in shallow mines that experience low horizontal clamping forces (Daehnke, et al., 2001). The zone can create a deadweight which can lead to potentially large collapses. This leads to the theory that shallow mines require more intense support than deeper mines. The calculated tensile zone is often utilized as the back area fallout thickness where there is insufficient data on which to base the fallout thickness. The lack of face

fracturing in shallow mines due to the relatively low stress levels (Figure 2.2) reduces the amount of dilational stresses. The horizontal stresses help to create a self-supporting beam (Jager & Ryder, 1999). The failures also occur along geological discontinuities or keyblock failure which causes unravelling.

The tensile zone is utilized in the support design at North Shaft where inadequate fallout data is available for the back areas of the stopes.

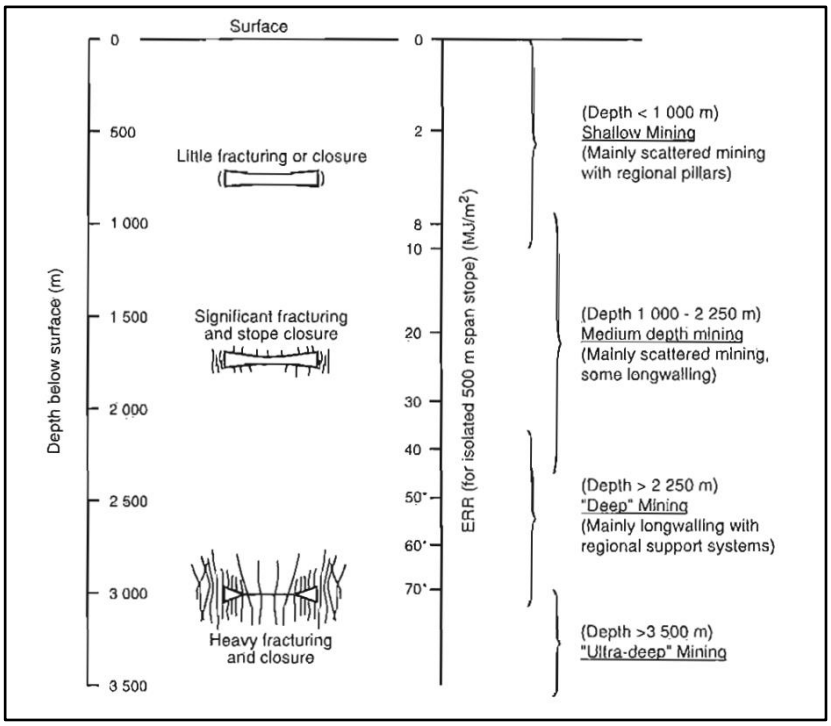

Figure 2.2: Variation in mining environments with depth (Jager & Ryder, 1999).

Various examples of tensile zone calculations are given in Figure 2.3 below. The tensile zone is greatest at shallow depths and decreases in height as the depth increases (Jager & Ryder, 1999).

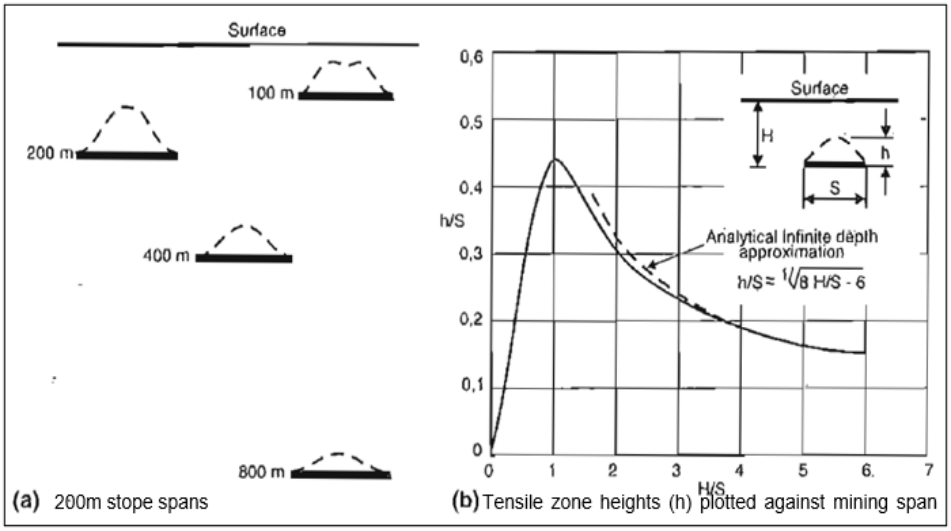

Figure 2.3: Tensile zone above shallow stopes at various depths (Jager & Ryder, 1999).

2.5 Key Concepts, Theories and Studies

The following section looks at some of the key concepts regarding pillar design, elongate support performance and closure measurement.

2.5.1 Regional Pillar Design

Pillars are used to stabilize the hangingwall strata. It is a generally accepted rule of thumb that regional spans be no more than half the mining depth. Regional pillars are designed for areas of geolosses. Bracket pillars along prominent geological structures can also act as regional support if they are wide enough (Figure 2.4). These pillars must have a width:height ratio greater than 10:1.

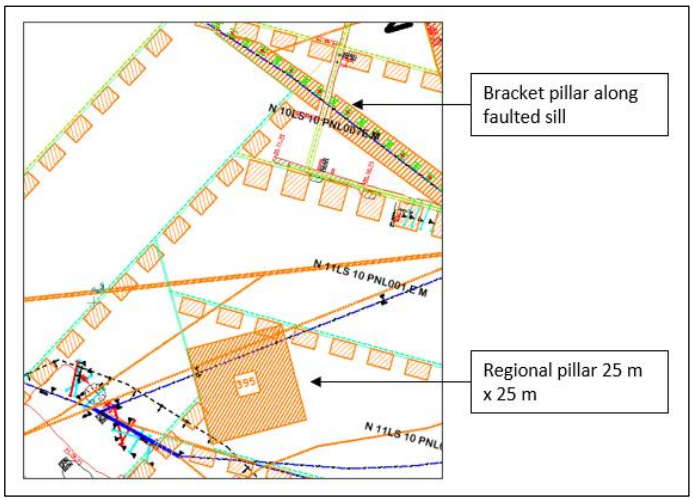

Figure 2.4: Regional pillar and bracket pillar.

The pillar design requires two main components to evaluate the stability of a pillar. The first is the pillar strength and the second is the load acting on the pillar (York, et al., 1998). The average pillar stress is calculated according to TAT (Figure 2.5). The main factors are the depth, pillar width and span. Regional pillar designs are generally conservative in nature due to additional ground lost along geological discontinuities and potholes.

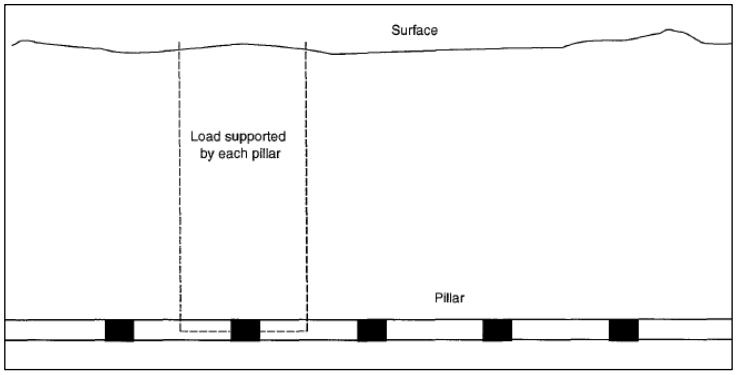

Figure 2.5: Tributary Area Theory demonstration of load attributed to each pillar (York, et al., 1998).

2.5.2 Crush Pillar Design

Designs are generally based on empirical experience and strength formulae derived from other ore bodies. This leads to oversized pillars and reduced extraction. Oversized pillars at deeper levels can lead to pillar bursts. Crush pillars are required to fail within close proximity of the face. The residual strength provides

the strength to support against backbreaks (Watson, et al., 2010). The design of an ideal pillar system was rationalised into a flowchart (Figure 2.6) by Watson et al. (2010).

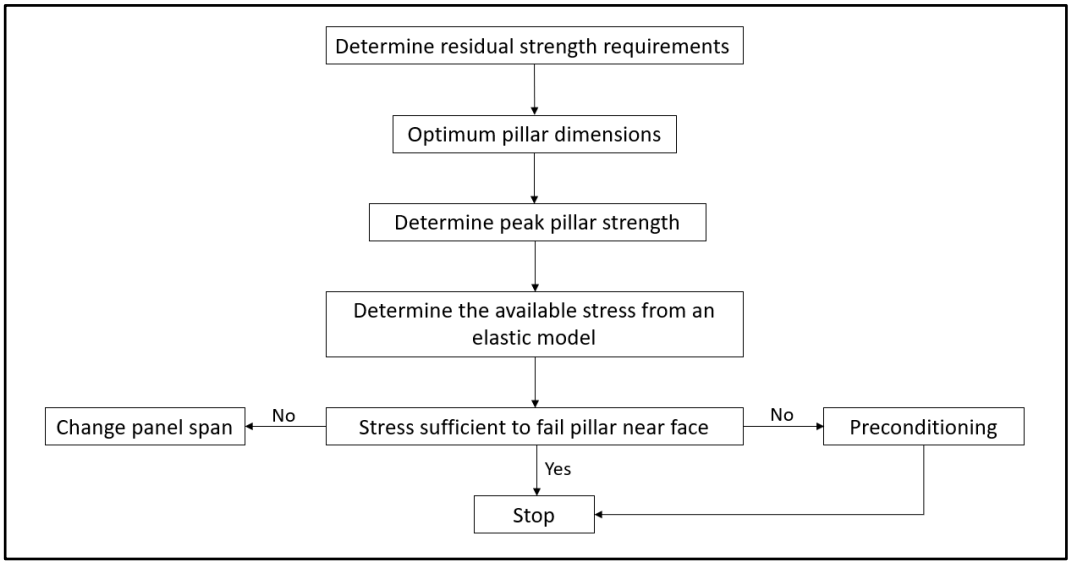

Figure 2.6: Flow chart for crush pillar design (Watson, et al., 2010).

At stope widths of 1.0 m to 1.8 m, the pillar width to height should not exceed 2:1. Beyond this, the pillar doesn't fracture in the stope face and can burst. A graph of residual average pillar stress versus width:height ratio was created by Watson et al. (2010). The graph compared measurements conducted with laboratory tests and numerical models to show good correlation with the approximate design (Figure 2.7). With width to height ratios of less than 2:1, any poor pillar cutting could lead to pillar failures. (York, et al., 1998).

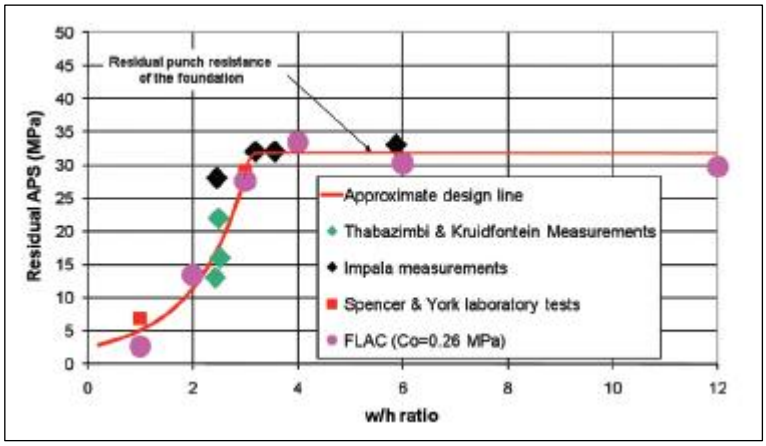

Figure 2.7: Pillar residual strength as a function of w/h ratio (Watson, et al., 2010).

An empirical formula was developed by Watson, et al. (2010) to compare against the Hedley and Grant formula in Equation 2.2. The difference in pillar height along the gully is catered for with a formula determined by Roberts, et al. (2005) in Equation 2.3. The h_e represents the gully, cut along one side of the pillar which creates one high side and one short side of the pillar.

$$Strength = 136[\frac{1.27}{1+\frac{0.27w}{L}}](0.59 + 0.41\frac{w}{h_e}) \qquad \textbf{Equation 2.1}$$

$$h_e = [1 + 0.2692(w/h)^{0.08}]h \qquad \textbf{Equation 2.2}$$

The pillars from the study showed a good correlation to the formula for the calculation of peak pillar strength (Figure 2.8).

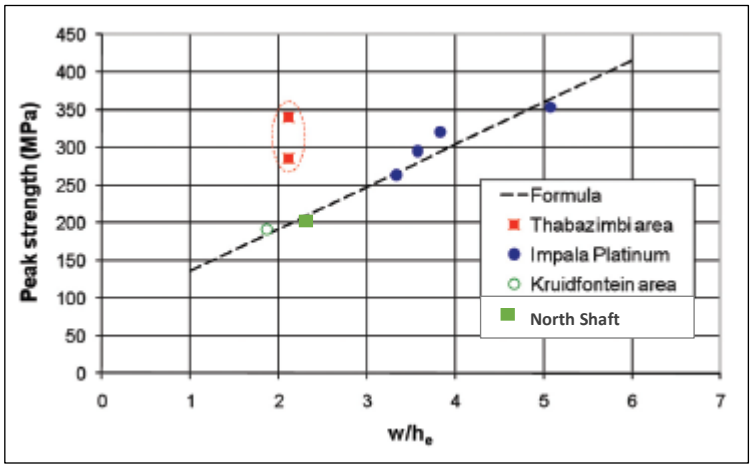

Figure 2.8: Comparison of the formula and measurements of peak pillar strength (Watson, et al., 2010).

The North Shaft pillar design falls along the estimated design line and underground observations of the residual strength of crush pillars are between 13 MPa and 25 MPa (Roberts, et al., 2005). This falls in line with the pillar residual strength estimations conducted in Figure 2.8.

2.5.3 Underground Elongate Performance Versus Laboratory Performance

Elongate support strength can be affected by a range of factors including the condition of the timber and quality of installation. The temperature and humidity underground can affect the behaviour of the elongates. Blast and scraper damage are a common occurrence underground. The most effective way to determine the elongate performance would be through underground measurements (Piper, et al., 2007).

The performance of elongates has been routinely tested in the laboratory under standard loading conditions however the performance consistency underground has not been properly evaluated (Daehnke, 2001). Work was conducted under SIMRAC project GAP 330 to allow for statistical analysis.

The testing protocol includes:

- Ten compression tests at a rate of 15 mm/min;
- Five rapid displacement tests at a rate of 3 m/s; and
- Five underground tests using load cells and closure loggers.

The SIMRAC project concluded that performance curves (Figure 2.9) could be created to ensure that a minimum of 90% of the support units exceed the support specification (Daehnke, 2001).

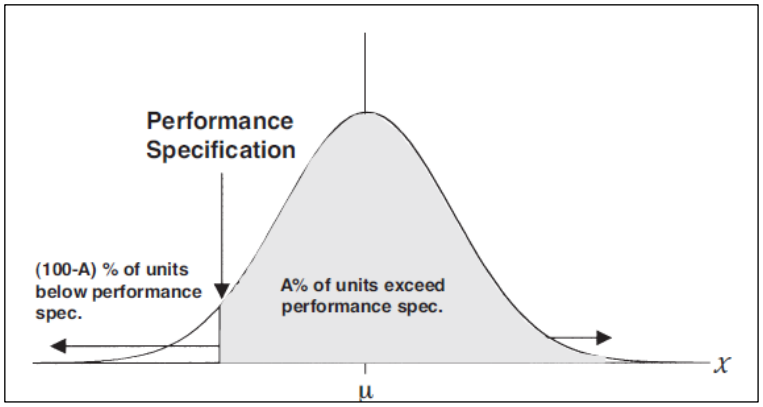

Figure 2.9: Probability density function sectioned according to performance specification (Daehnke, 2001).

2.5.4 Closure Measurement

Observational methods such as closure logging can be used during mining. The analysis of the ground-support interaction is the only way to verify the excavation designs that were based on empirical and analytical methods (Swart, 2005). Closure measurement data was recorded with closure loggers (Figure 2.10). The data can be used as a predictor for large collapses in mines. Closure data can also be used for improving support designs through the inclusion of the effect of the mining rate (Malan & Napier, 2021). The data can be used to define ground control districts with specific support strategies.



Figure 2.10: Closure logger installed in a stope panel.

2.5.5 Historical Closure Studies

A study was conducted on shallower levels with closure logger and extensometer instrumentation. An extensometer measured up to 7 mm of dilation between 10 – 15 m in the hangingwall. The cause was inferred to be separation along the Bastard Reef but was not confirmed with further investigation (Malan, 2007). The closure measured was close to zero on six of the panels (Figure 2.11) but one of the six panels did show a closure of 6 mm over the two month duration of the study (Malan, 2007). This was well within the support yield capacity of the mine poles.

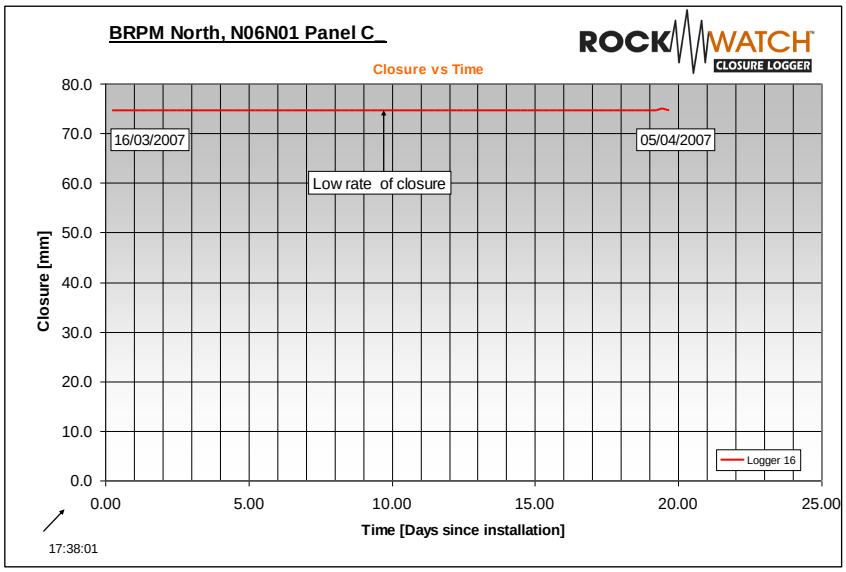

Figure 2.11: Historic closure measurements conducted on the Mine (Malan, 2007).

2.6 Key Debates

2.6.1 Geological Discontinuities

Bedding planes or partings in the hangingwall can cause widespread closure if they are located high enough in the hangingwall. The main contact of concern is a chrome stringer known as the 'Bastard Reef' at 9 – 15 m above the Merensky Reef highlighted with a red square in Figure 2.12. The contact can have a shear plane. The similarity to the Merensky reef chrome stringer means that it has often been mistaken to be the Merensky reef but it has no significant PGM value. A parting is found between the Merensky hangingwall pyroxenite and the hangingwall norite/anorthosite is highlighted with a red square, this parting is generally located between 2 – 3 m into the hangingwall.

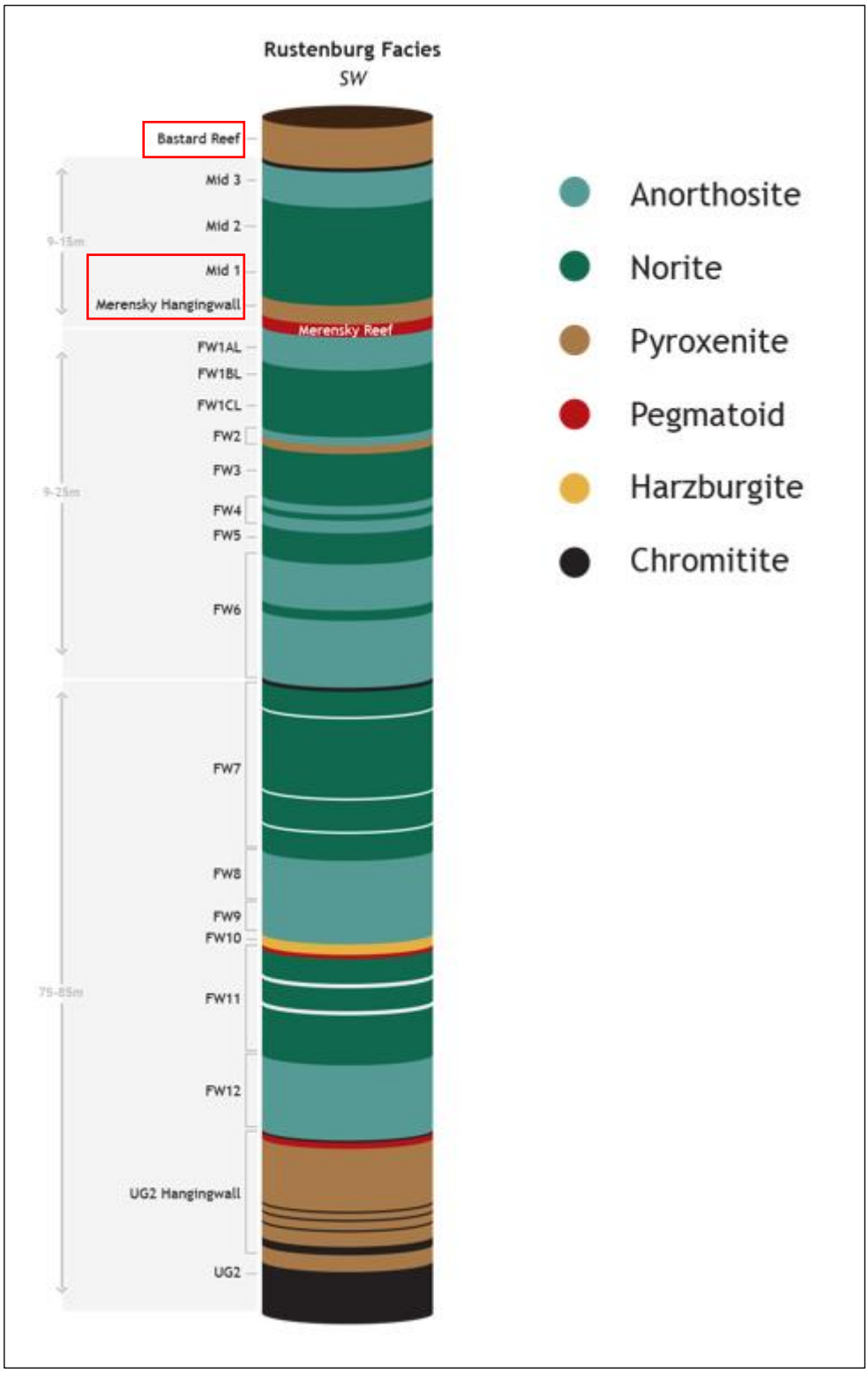

Figure 2.12: Stratigraphic column of the BRPM mining locality (Impala Bafokeng - Geology Department).

The stability of the panels is influenced by the geological discontinuities present. The discontinuity spacing, infilling, orientation, dip and persistence all factor into the overall stability. A typical wedge failure is presented in Figure 2.13 below. Dome structures or curved ramp structures occur randomly and have been observed to extend from as little as 2 m to as much as 30 m across a panel. Investigations of numerous FOG's by York et al. (1998) found that almost all the FOG events were linked to major geological discontinuities and not due to span alone. They found that there was a correlation between a reduction in span and improvement of hangingwall conditions where shallow dipping discontinuities were present.



Figure 2.13: Wedge failure between joint sets.

2.6.2 Rock Mass Rating Systems

A need was identified for a methodology to design stable spans in combination with appropriate support systems. The system would need to work in a variety of rock mass conditions for the duration of the mining period (Watson, 2004). The available rock mass rating systems were found to be inadequate for describing all the geotechnical conditions and failure mechanisms observed on the Merensky Reef. A new system was proposed and termed the 'New Modified Stability Graph' (N") system (Figure 2.14). The system combines the Q-system for rock mass characterisation, the Stability Graph method and the Impala Platinum rating system. The system caters specifically for span and support design on the Bushveld mines (Watson, 2004).

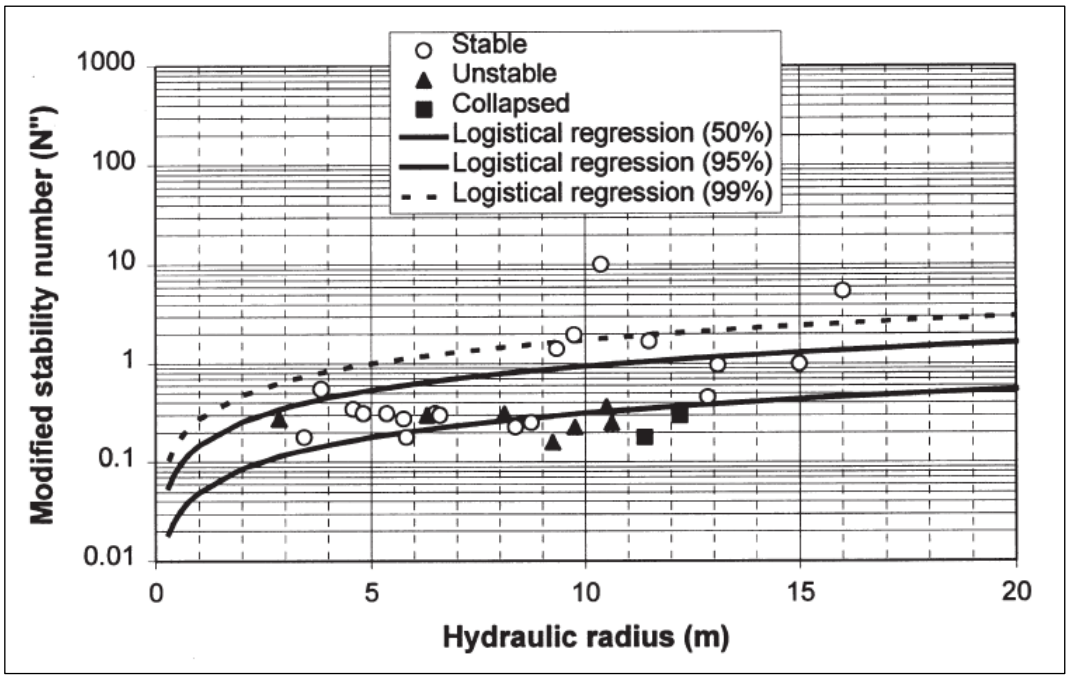

Figure 2.14: New modified stability graph plot of stopes supported on mine poles with a support resistance of 128 kN/m^2 (Watson, 2004).

2.6.3 Numerical Modelling

Due to the difficulty and costs involved in obtaining underground data, many studies are conducted using estimated input values. Modelling can be a useful tool for verifying designs but it cannot be relied upon in isolation. If the information that is entered into the model is incorrect or inadequate, the answers may lead to the wrong design being implemented. This has been referred to as 'geotechnical assessment deficiencies' (Malan & Napier, 2021). This is the difference between modelled behaviour and the actual behaviour of the rock mass. The steps leading to the data collection are often more important than the model itself (Stacey, 2009). If the data collection is not conducted diligently and accurately, the model will be based on poor inputs and would lead to an inaccurate output.

Elastic analysis can produce inaccurate estimates of stope closure as time-dependent closure can continue for weeks after blasting has been stopped (Malan, et al., 2007). Monitoring data can lead to unexpected findings about the rock mass behaviour that may not fit the numerical modelling as expected (Malan & Napier, 2021). Time-dependent closure data can indicate whether the crush pillar design

is behaving as expected. If closure is not identified then, it may be an early indicator of potential pillar bursts (Malan & Napier, 2021).

The panel span, stope span and pillar width are critical to the loading system in shallow and intermediate mines. York, et al (1998) recommend modelling with the finite depth approach. Finite depth approach considers the effect of surface loading on the model according to a ratio of stope span to depth. At ratios greater than 0.25, the rock mass experiences bean bending and the tensile zone also has an effect which must be considered. They noted that the length of the surface modelled should be > 5 times the mining span.

2.6.4 Accuracy Of Underground Measurements

The position of the closure logger is critical when attempting to measure closure. It can lead to incorrect closure rates being measured due to the rapid decrease in closure rates as the distance to the face increases (Malan, 2003). As seen in Figure 2.15, the recorded rate of closure decreases significantly the further away from the mining face that the instrument is installed. A logger that is installed at 20 m from the face, would record a much lower rate than a unit installed at 1 m from the face. The risk of damage to the closure logger increases with proximity to the face area. The damage could be due to fly rock from the blast. Mechanical damage can also be caused by scraper interaction or pipes being moved for drilling. A compromise is required between the most accurate measurement and the lowest risk to the equipment. The loggers were installed between 10 and 12 m from the face to be behind the last line of sweepings. The chance of scraper and fly rock damage was greatly reduced.

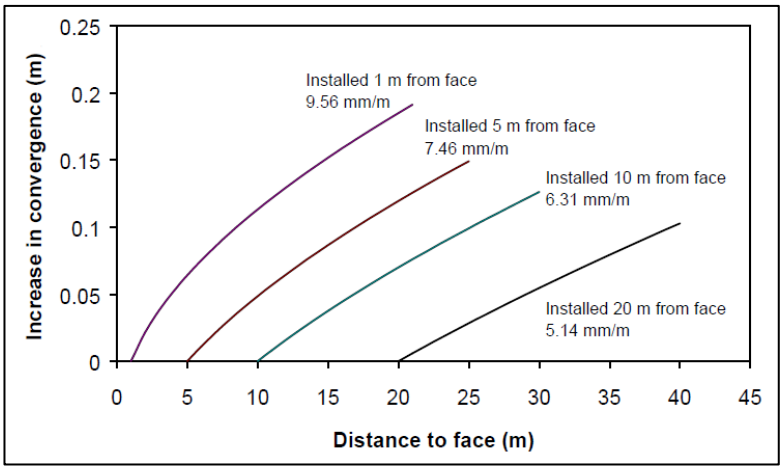

Figure 2.15: Calculated convergence rates based on closure loggers installation position (Malan, 2003).

Closure measurements can be conducted using closure pegs, with measurements conducted manually during visits to the workplace. A vernier closure meter is installed between a hook and the peg and readings measured on a ruler (Figure 2.16). Measurements must be taken more regularly to obtain a rate of closure.

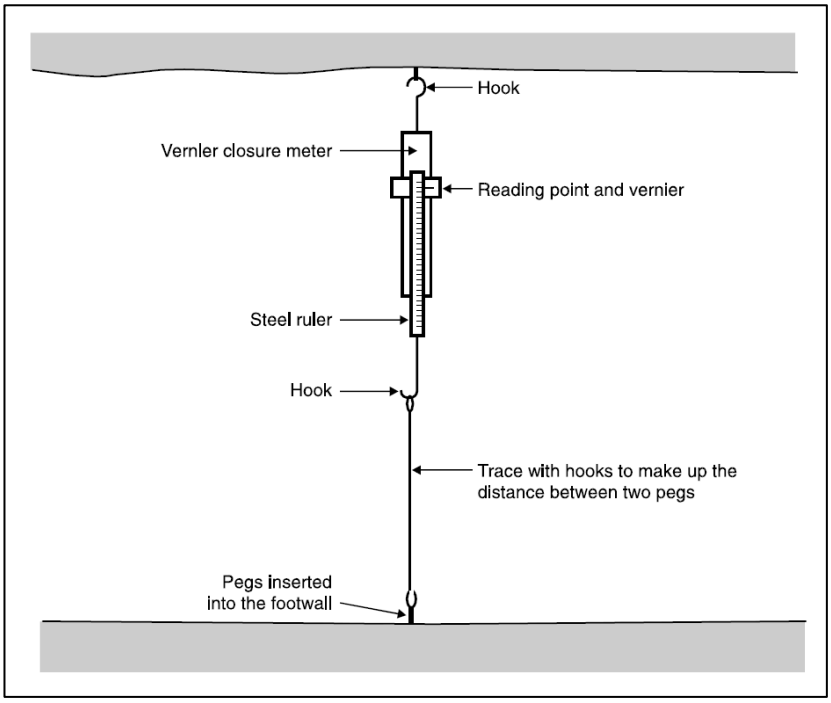

Figure 2.16: Manual closure measurement tool (Jager & Ryder, 1999).

Manual measuring can lead to a loss of important data such as the rate of closure after a blast (Malan, 2003). The initial rate of closure after blast is high. The closure rate then takes place as a steady state until the next blast (Figure 2.17).

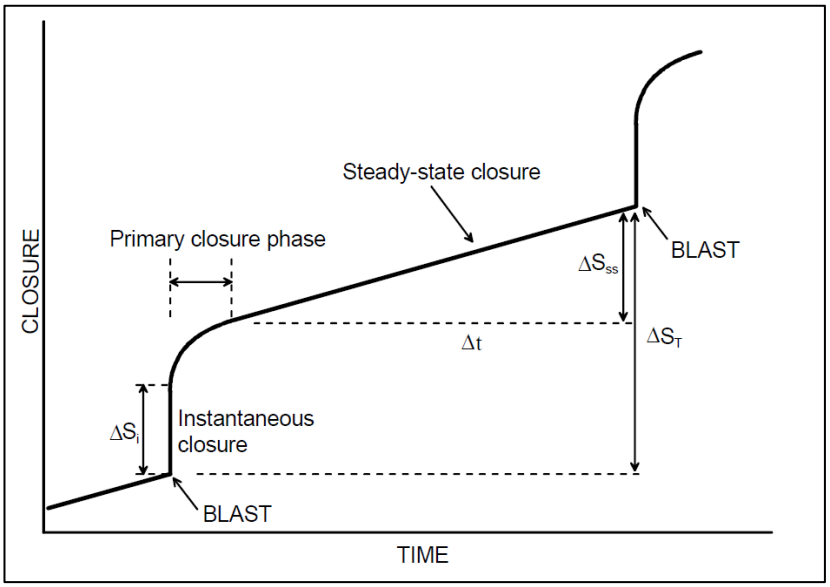

Figure 2.17: Continuous closure measurement and typical terms used (Malan, 2003).

2.6.5 New Monitoring Techniques

The measurement of closure has generally been conducted with closure loggers, tape extensometers or extensometers. The data would be applicable for a specific point in the stope and may not necessarily represent the deformation along the entire excavation. Recent advances in the use of Light Detection and Ranging (LiDar) where successive images are superimposed on each other was applied by Jones & Beck (2017). The data allowed for a more comprehensive understanding of the direction, extent and magnitude of the movement (Figure 2.18). The scans can differentiate between different parts of the excavations being stable, converging and diverging over time (Jones & Beck, 2017).

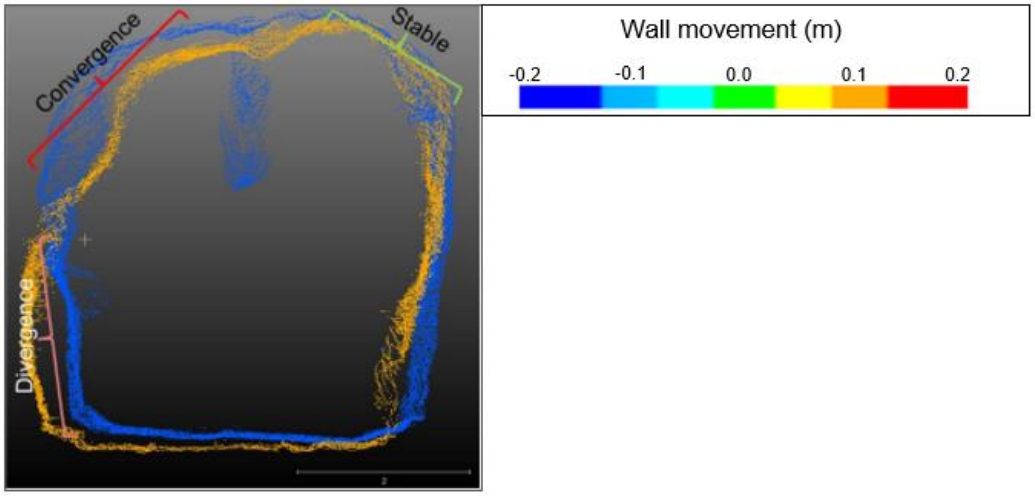

Figure 2.18: A cross section of a drive showing deformation that has taken place (Jones & Beck, 2017).

The combination of borehole camera and GPR to monitor the internal pillar yielding behaviour was conducted at South Deep Mine. The fracturing depth could be measured in relation to the support design and pillar failure processes (Figure 2.19). The information was used to confirm the pillar state and whether there was a risk of pillar bursts (Andrews, et al., 2019). The effectiveness of face preconditioning could also be assessed.

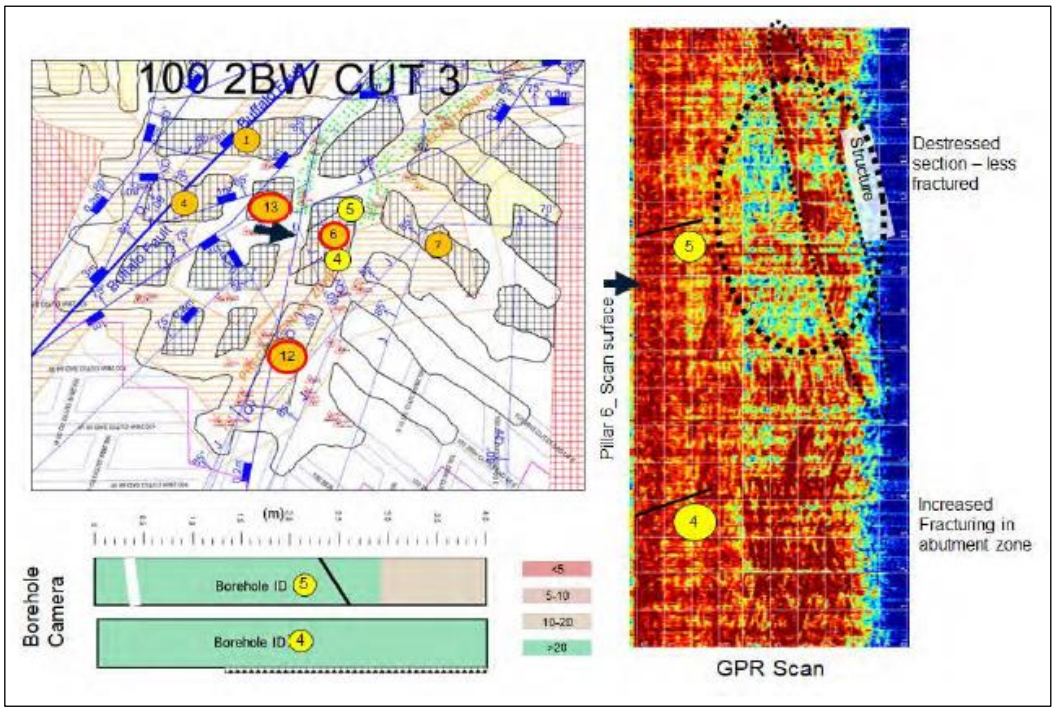

Figure 2.19: GPR scans and borehole camera correlation on pillar (Andrews, et al., 2019).

2.6.6 Neighbouring Mine Case Study

A study was conducted on a neighbouring Impala Mine to understand the rockmass and pillar behaviour. The mine selected was the No.10 Shaft which was mining Merensky reef. The stoping width, pillar sizes and reef dip are well matched to those of North Shaft. The test site was deeper than current North Shaft workings, at 930 m below surface. Closure measurements conducted simultaneously with stress measurements on a pillar found that pillar yield corresponded with footwall heave next to the pillar (Lougher & Ozbay, 1995).

The pillars were modelled with FLAC to have a peak strength of 150 MPa (Le Bron, 2015b). The footwall anorthosite (144 MPa) is weaker than the hangingwall pyroxenite (170 MPa) (Lougher & Ozbay, 1995). Fractures of the footwall were observed. The pillar loading caused high horizontal stresses in the footwall between the pillars. The Footwall 4 contact is formed along an infilled layer and creates a parting plane, forcing the stresses to move horizontally. The footwall thrusts into the stope and overcomes the limited yield capability of support units. The study found that support resistance of the pillars was adequate for the hangingwall stability up to the Bastard Merensky parting.

2.6.7 Pillar Behaviour

The original Hedley and Grant study that formed the pillar strength formula was conducted on rock types different to those in South African mines. It has been found that the formula may underestimate pillar strength (Malan & Napier, 2011). Tributary area Theory can overestimate the load acting on pillars by over 25% (York, et al., 1998). This could lead to oversized pillar designs.

Variations in pillar strength can be caused by three main factors as described by York et al. (1998):

- Differences in stoping width and pillar dimensions which leads to the overall w:h ratio;
- The strength of the pillar material; and
- Sheared or infilled contacts between the pillar and the hangingwall or footwall which could lead to slip and a weakening of the pillar.

Other factors that have localised influence are:

- Weak layers within the pillars;
- Varying heights of the pillar on different sides;
- Geological discontinuities within the pillar;
- Brittleness of the pillar material; and
- Loading rate (York, et al., 1998).

A preliminary chart for the design of crush pillars was created by York et al. (1998) as there was little other design material available for hardrock crush pillars (Figure 2.20). The design chart indicates that at depths up to 600 m, with 3 m wide pillars, the mine pillar design falls into the crush pillar category.

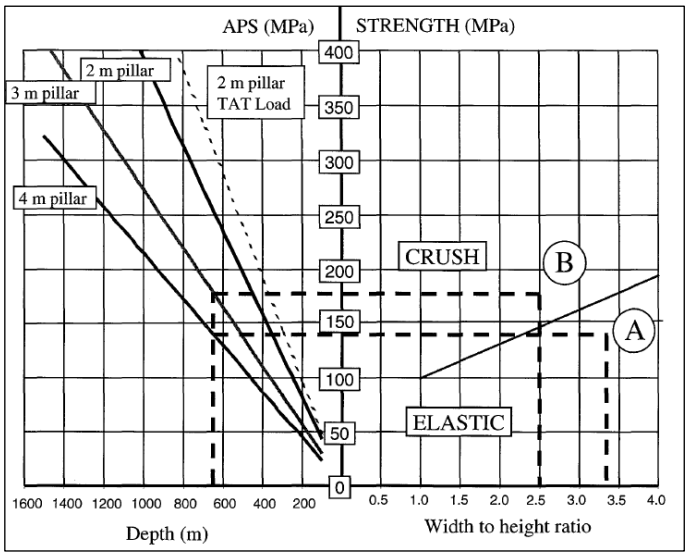

Figure 2.20: Design chart for crush pillars (York, et al., 1998).

3 RESEARCH METHODOLOGY

A quantitative research methodology was designed to reduce the uncertainty regarding closure that was observed. A combination of primary data collected from instrumentation, closure monitoring and visual observations was planned. The monitoring data was used to check whether the initial design was valid.

3.1 Closure Logger Studies

Historical closure measurements were conducted in 2007 after a large fall of ground (FOG) took place in the upper section. Loggers were installed in 8 panels across 5 and 6 Levels (Figure 3.1). Very low closure was measured for the panels that were investigated. Low closure was expected at depths of less than 400 m.

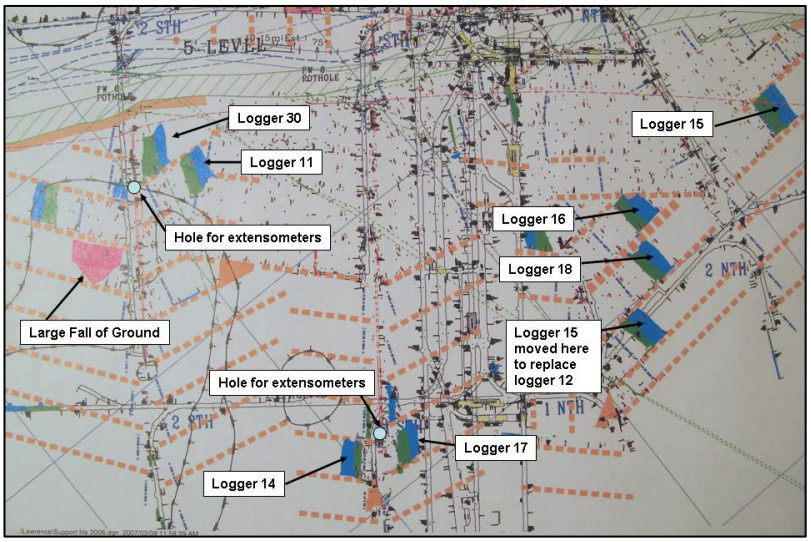

Figure 3.1: Location of closure loggers installed on 5 and 6 levels (Malan, 2007).

3.2 Research Design

Instrumentation work was the main area of focus for investigating the closure rate and whether there were any weak partings in the hangingwall. The instrumentation was conducted around the area of the observed support failure and towards future mining areas to determine the persistence of the high closure. Visual observations and investigations were also conducted to assess the falls of ground that had occurred in the area and to inspect pillar behaviour and panel spans.

Current working panels were required for the study. Closure loggers were purchased from Groundwork Consulting. The measurement of closure with advance was the focus. The installation process is captured in Figure 3.2 below.



Figure 3.2: Closure logger installation by the author.

The loggers were used to determine the rate of closure per metre of advance. A total of 5 loggers were installed across the working places (Figure 3.3). The locations of the closure logger units were captured on Microstation. The panels selected were within the area where high support failure was observed. The location, reference numbers, and date of installation of the loggers were plotted on Microstation.

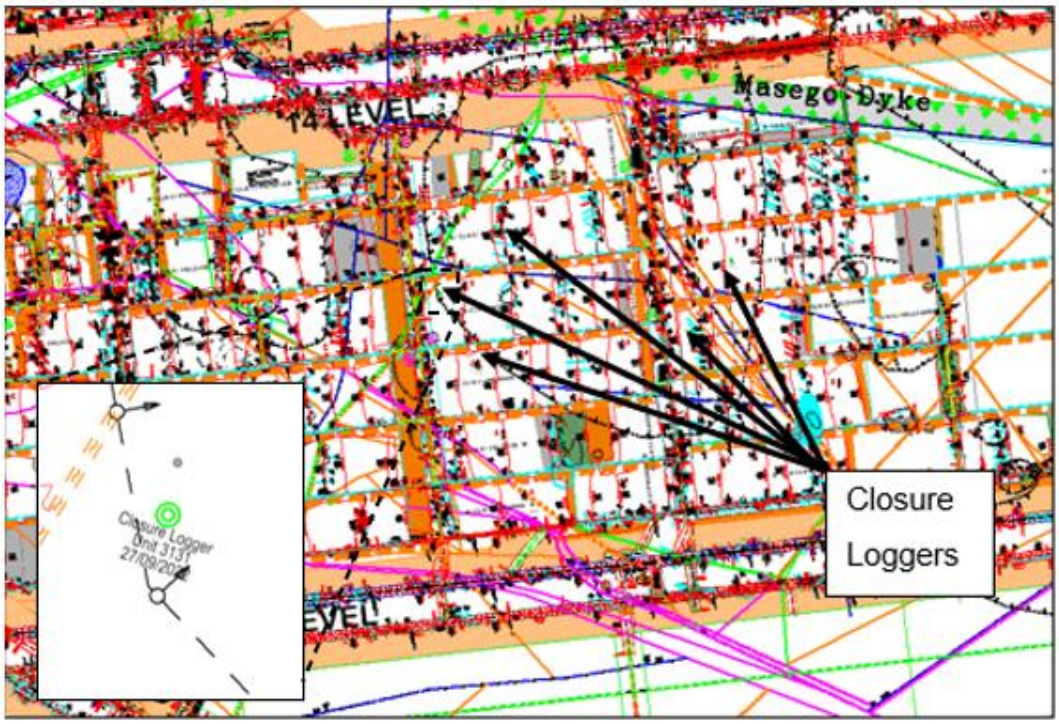

Figure 3.3: Closure Logger installations plotted on plan.

3.3 Borehole Camera Observations

Borehole camera work (Figure 3.4) was conducted along the Roadways. The location of the holes was limited to locations where the Geology Department was drilling cover holes. The holes were drilled vertically to a depth of 15.0m into the hangingwall. The 15.0m depth was chosen as this was the known depth of the Bastard Reef chrome parting.



Figure 3.4: Rock Engineering Department borehole camera.

The first hole was up-dip from the 15 level stopes of interest, along the 14 Level Roadway. The second hole was drilled down-dip from the 15 level stopes, along the 15 Level Roadway. The boreholes were requested to be drilled to the Bastard Reef contact to check for any tensile failures. The number of holes drilled was limited due to production pressure to cover the development ends.

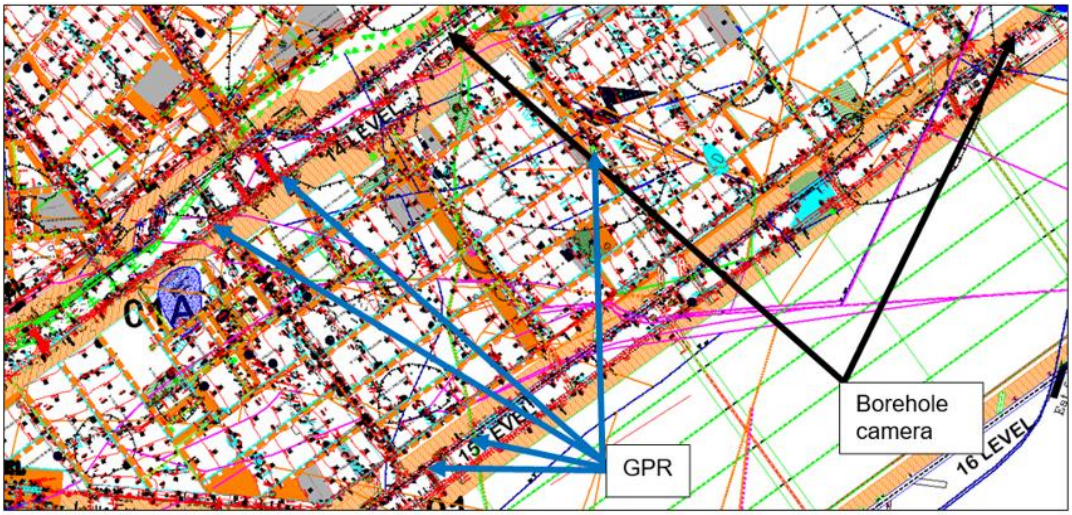

Figure 3.5: Instrumentation locations for the initial study.

3.4 Ground Penetrating Radar

GPR scans were planned along the 14 and 15 level roadways and along the 15 level north 2 raise line. The roadway scans were near the boreholes (Figure 3.5). The borehole camera work was used to compare with the GPR scans. Any observations on the scans were be referenced against physical observations.

Ground penetrating radar (GPR) utilises electromagnetic pulses generated from an antenna which then reflect off surfaces. Any change in the electrical properties of the rock mass present forms a positive reflection (Figure 3.6) (Pienaar, 2017). The reflections of the pulses could be rock contact changes, fractures or geological discontinuities. The reflections are then detected by the antenna on their return and as the user walks along with the unit. This creates a profile of the area that was scanned.

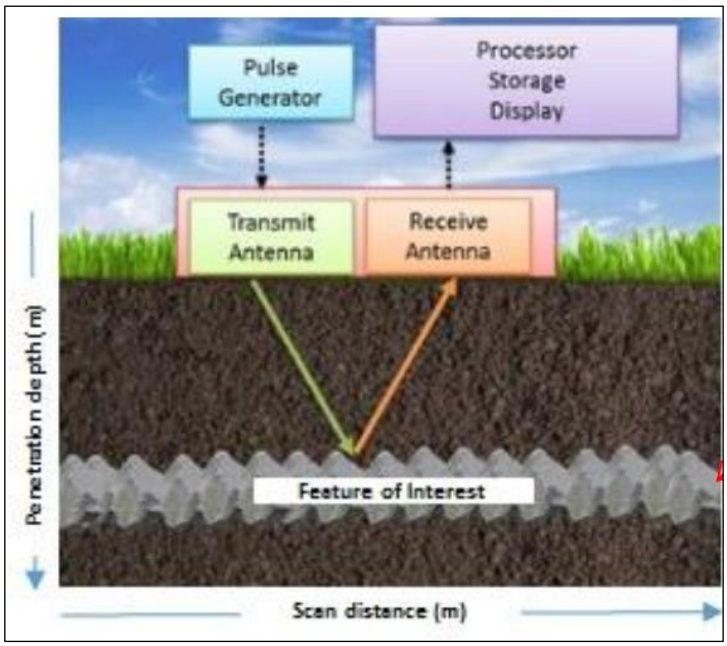

Figure 3.6: Simplified system block diagram of a GPR system (Pienaar, 2017).

The GPR that was utilised is referred to as a Sub Surface Profiler (SSP). The unit was purchased from Reutech. The author's experience with previous GPR systems was challenging. Older systems were bulky, heavy, and very complex to use. The data would not be available to assess until processed on surface. The SSP is lighter and wireless. The tablet enables the user to check the scans immediately (Figure 3.7). Technology that is more user-friendly enables scans take place more regularly.



Figure 3.7: Sub Surface Profiler used for GPR analysis (Andrews, et al., 2019).

3.5 Visual Observations

Visual observations were conducted for the in-stope pillars to determine whether they were behaving as expected according to the crush pillar design (Figure 3.8). Observations were conducted to inspect the footwall and hangingwall for fracturing. Panels were identified on plan with various spans and then visited to assess the support behaviour in the workplaces identified. The spans ranged from 24 m to 30 m. Back analysis of falls of ground were conducted to verify the failure mechanisms involved.



Figure 3.8: Crush pillar scaling at N15 Level.

4 RESULTS AND DISCUSSION

4.1 Data Collection Process

The process of collecting the data is detailed below. The methods include database analysis of FOG's and visual observations of panels and pillars underground. Laboratory testing of support units and underground experimental support trials were conducted. Instrumentation was conducted through various different tools and results compared across the methods.

4.1.1 FOG Back Analysis

The failure mechanism of the FOG's that have occurred in the section were analysed. The dead weight fallout of keyblocks or wedges was the main mechanism observed. Unravelling was observed but would occur after the elongate failure had taken place and the required support resistance was no longer provided. The C-Packs would prevent unravelling and compartmentalise the falls (Figure 4.1).



Figure 4.1: FOG along C-packs prevented further unravelling.

Analysis of the FOG database from 2019 to 2023 was conducted (Figure 4.2). The results indicate that domes were present in half of all falls of ground that were investigated in the section. Low angled joints with a dip of less than 40° were present in 56% of all FOG's.

In the panels where support failure has taken place, there has been no complete hangingwall unravelling. The failures have taken place along geological structures such as shears, faults and domes.

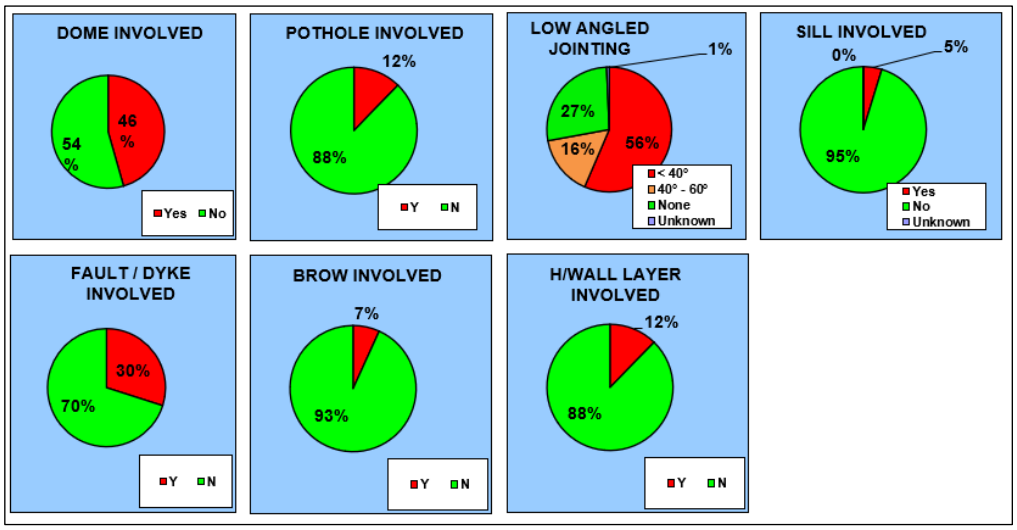

Figure 4.2: Breakdown of FOG's from 2019 - 2023 by geological discontinuity (Impala Bafokeng FOG database).

4.1.2 Closure Logger Data

Data from the closure loggers was collected twice a month. The data was collected from the loggers using a tablet which acted as a data grabber. The tablet is equipped with a Bluetooth system. This allowed the data to be collected safely without having to enter the back areas of the panel.

4.1.3 Borehole Data

The data collection for the borehole camera was conducted by the author, accompanied by a strata control officer. The borehole camera had an onboard recording system which was used to record video of the holes that were assessed (Figure 4.3). The data is then transferred to the server using an SD card reader.

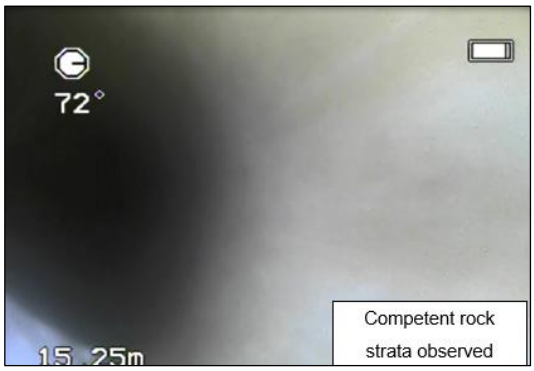

Figure 4.3: Screenshot taken from borehole camera investigations.

The borehole core was drilled and brought to surface by the drilling contractor. The core was then logged by the Geology Department on the Sable core logging program.

4.1.4 Visual Observations

Data collection for visual pillar observations and comparisons of different panel lengths were conducted. A team of mining and rock engineering personnel was formed to ensure that safety was prioritised whilst accessing the back areas of the stopes. All reported FOG's were investigated and failure mechanisms were observed.

The crush pillars were inspected and appeared to be behaving as designed (Figure 4.4). No sign of any pillar failure was found. Scaling was observed as expected but the pillar cores remained stable. The taller gully sides of the pillars, along the advanced strike gully (ASG) showed less scaling than the shorter side at the top of the panels. The gully sidewalls were bolted to reduce scaling which increased the confinement on this side.

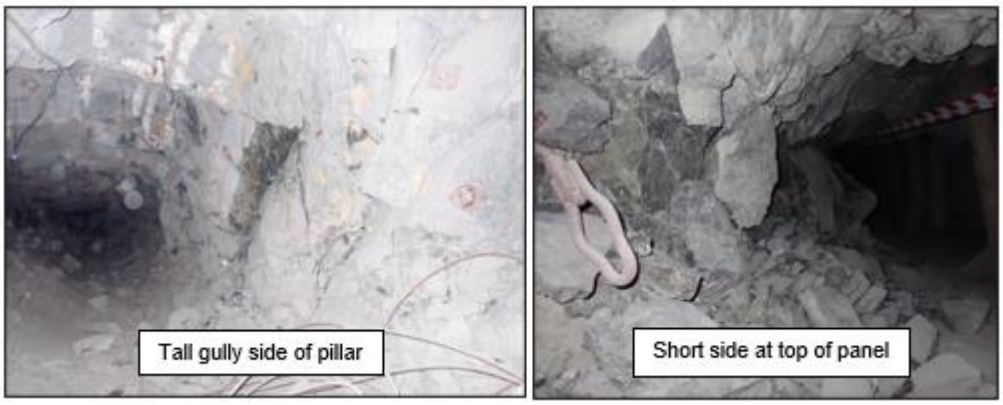

Figure 4.4: Pillar observed during underground investigations.

A mined-out panel was visited to check the footwall and hangingwall condition around the crush pillars. The pillar selected (A) measured 6.3 m in length and an average of 3.5 m in width. The pillar is indicated in Figure 4.5 along with the position of tensile cracks and footwall shearing observed.

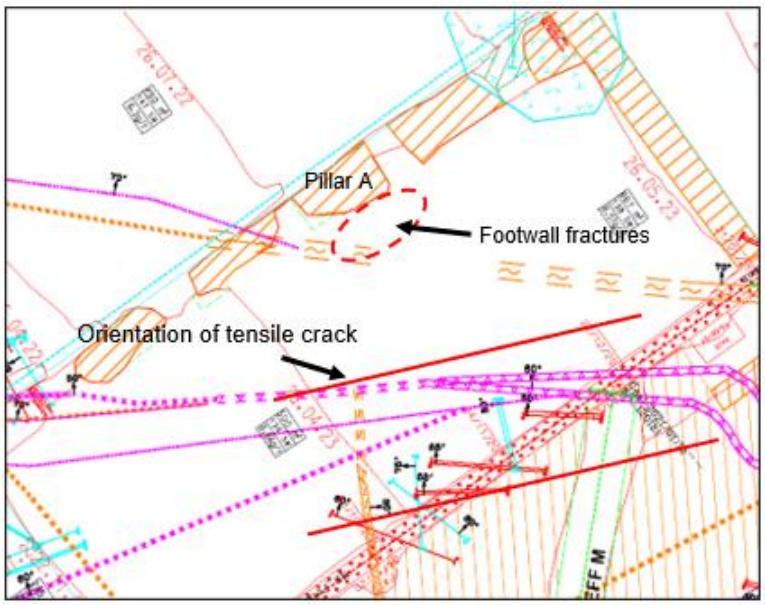

Figure 4.5: Location of pillar observed.

The hangingwall around the pillars was observed to be competent and no fractures were present (Figure 4.6). Hangingwall conditions were stable.



Figure 4.6: Hangingwall condition around the crush pillar.

The footwall around the pillars had fractured significantly and fresh fractures had formed. Significant footwall heave had taken place within approximately 3 m proximity to the pillar (Figure 4.7).



Figure 4.7: Footwall fracturing and heave around a crush pillar footwall.

Tensile cracks were observed in the footwall of the panel. The tensile cracks measured had an 8 mm aperture and extended for a trace length of more than 20 m (Figure 4.8). The tensile cracks were orientated near parallel with the mining direction.



Figure 4.8: Tensile cracks in the footwall.

4.1.5 GPR Data

GPR scans were conducted on both 14 Level and 15 Level Roadways as they are on reef excavations and located on either side of the closure areas. The GPR was used to correlate the findings of the borehole camera work conducted (Figure 4.9). The profiles are recorded directly to the tablet and then transferred to the server via Bluetooth. Additional scans were conducted along the 15 Level north 02 raise line.



Figure 4.9: The author conducting GPR scans along the Roadway.

4.2 Data Validation Process for Closure Loggers

The data for the closure loggers was sent to the OEM Supplier to ensure that it was processed correctly and to ensure that valid data was used for the analysis. The results were presented graphically in Figures 4.10, 4.11, and 4.12. Unfortunately, 3 of the 5 loggers were damaged, the cause of the damage was unknown. The figures represent the measured displacement in mm over time.

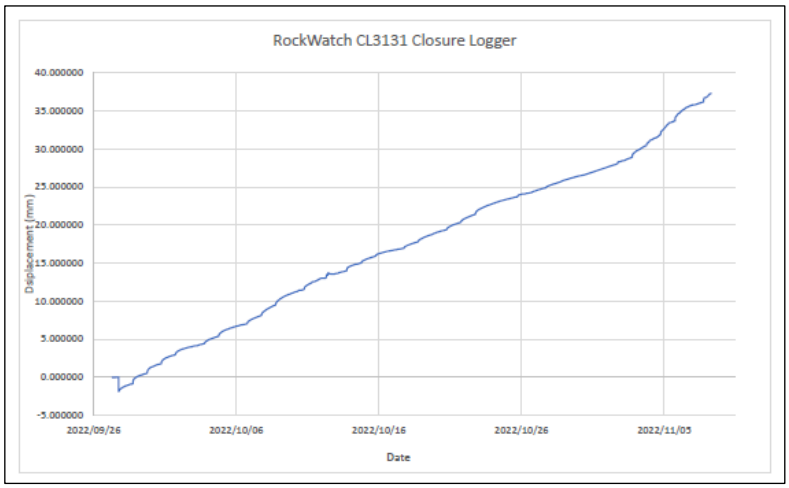

Figure 4.10: Closure logger data after 5 weeks (Unit 3131).

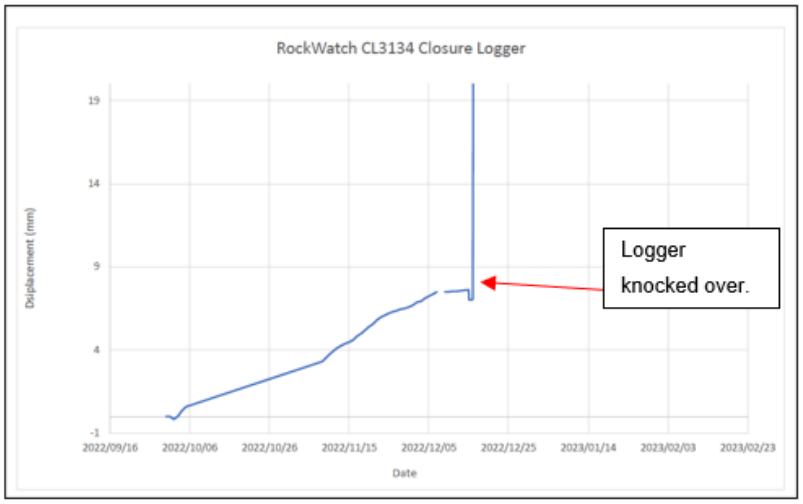

Figure 4.11: Closure logger data after 8 weeks (Unit 3134).

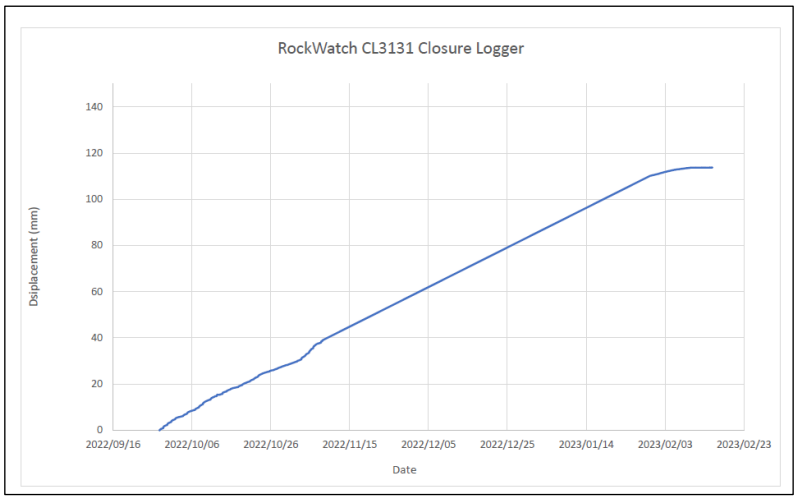

Figure 4.12: Closure Logger data after 5 months (Unit 3131).

4.3 Data Analysis Approach

4.3.1 Closure Data Analysis

The closure measured on the loggers between the periods of 26/09/2022 and 05/11/2022 was 38 mm. The advance over this period was 22 m. The closure measured was higher than would typically be expected at these mining depths.

$$\frac{Closure\ measured\ (38\ mm)}{advance\ (22\ m)} = Closure\ rate\ (1.72\ mm/m) \qquad \textbf{Equation 4.1}$$

The closure measured on the loggers between the periods of 26/09/2022 and 23/02/2023 was 115 mm. The advance over this period was 64 m.

$$\frac{Closure\ measured\ (115\ mm)}{advance\ (64\ m)} = Closure\ rate\ (1.79\ mm/m) \qquad \textbf{Equation 4.2}$$

The implication of the closure rates recorded is that the mine pole support units would reach their maximum deformation within 17 m face advance and would begin to fail.

4.3.2 Borehole Camera Correlation With GPR

Borehole data was compared with the GPR scans that were conducted. The GPR scans show no obvious parting besides the consistent contact at 2.0 m into the hangingwall (Figure 4.13). The contact was between the Merensky hangingwall pyroxenite and the Mid 1 Norite. The scans were analysed using the different tools available from the SSP software suite.

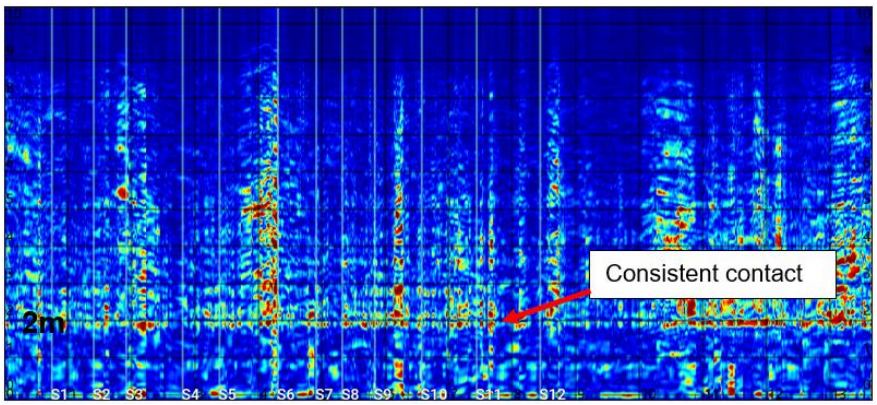

Figure 4.13: GPR scan of 14 Level Roadway.

The borehole camera was used to confirm the contact and a screenshot was taken from the video recording (Figure 4.14). The contact is generally weak and responsible for a large proportion of hangingwall stability issues (Lougher & Ozbay, 1995).



Figure 4.14: Contact from Merensky hangingwall to Norite.

4.3.3 Ground Penetrating Radar Analysis

The GPR scan of the raise line confirmed that there was no sign of instability in the immediate hangingwall beyond the previously observed parting at 2 – 3 m into the hangingwall (Figure 4.15).

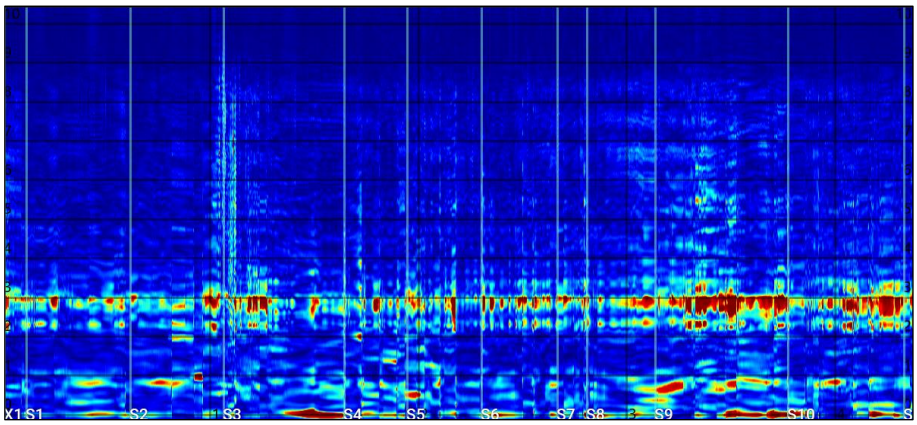

Figure 4.15: GPR scan of 15 Level north 02 raise line.

4.4 Changes to Support Strategy

The closure study was a lengthy process and an immediate support rehabilitation strategy was required to facilitate safe mining during the data collection and processing stages. C-Packs were selected to be installed in place of the 3-stick clusters as the back area support. C-Packs can withstand high loads and are a high yield support system. They permit a large amount of deformation before reaching their peak support loads (Figure 4.16).

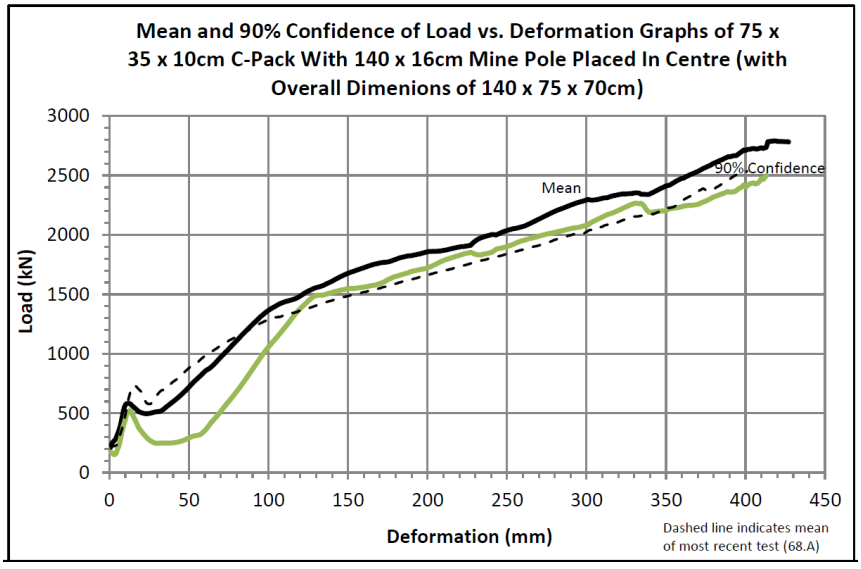

Figure 4.16: Load-deformation chart of C-Pack (Khosa, 2021).

The installation of C-packs is relatively simple but demanding in terms of logistics due to the number of segments required to build each pack (Figure 4.17). On a

mine with limited time available in the material decline, this led to transport difficulties but was introduced to all hybrid section panels that were mining at 30 m spans.



Figure 4.17: C-pack construction and testing at the CSIR Laboratory in Johannesburg.

4.5 Unturned Mine Poles Versus Pencil Sticks

Table 4.1 below shows the comparison between different diameter mine poles; the greater the diameter of the pole, the greater the ultimate strength. The peak load is then downrated to cater for the difference in loading rate from the laboratory to underground working places.

Table 4.1: Load capacities of mine poles (Khosa, 2022).

Ref. No.	Mean Diameter (cm)	Mean Peak Load (kN) (Excel Graph)	Mean Peak Load (kN) (Calculated)	Expected Range (kN)
45.G.1.1-5	17.6	606	683	365-608
45.G.2.1-5	19.4	894	905	443-739

The mine poles (18 – 20 cm) that are currently installed, reach their peak strength after a displacement of 30 mm (Figure 4.18). This means that after approximately 18 m advance, the closure caused the mine poles to fail.

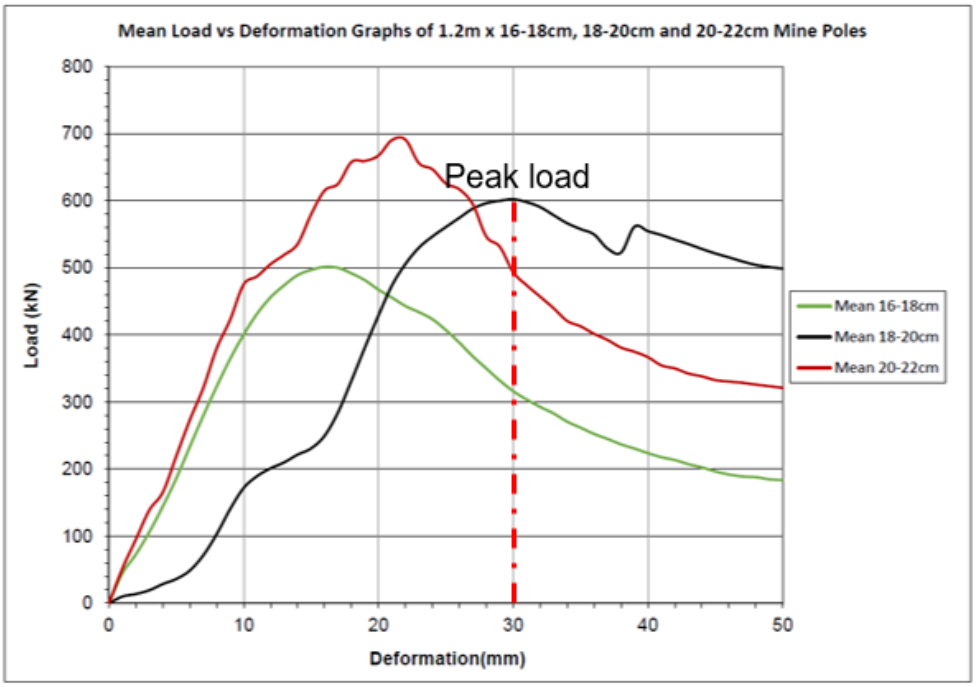

Figure 4.18: Load-deformation chart of various size mine poles (Khosa, 2022).

Pencil sticks were tested as an alternative to the mine poles. They provide the benefits of a stiff support system with the yielding capability required for the closure experienced. The profiled portion of the stick brushes/yields (Figure 4.19) in a controlled manner to allow the load to be shed whilst maintaining the support resistance. The strategy falls in line with those of industry experts: “The problem of premature failure of props caused by footwall heave, resulting from pillar punching, can be overcome by installing yielding elongates” (Jager & Ryder, 1999).



Figure 4.19: Pencil sticks selected for load deformation testing (Mabitsela, 2023).

Pencil sticks allowed for the support pattern and installation methods to be maintained. The total installation price is not increased due to a smaller pre-stressing device required. They are capable of rapidly reaching peak load, within 10 – 15 mm of deformation. The pencil sticks maintain that load for up to 120 – 150 mm of deformation (Figure 4.20).

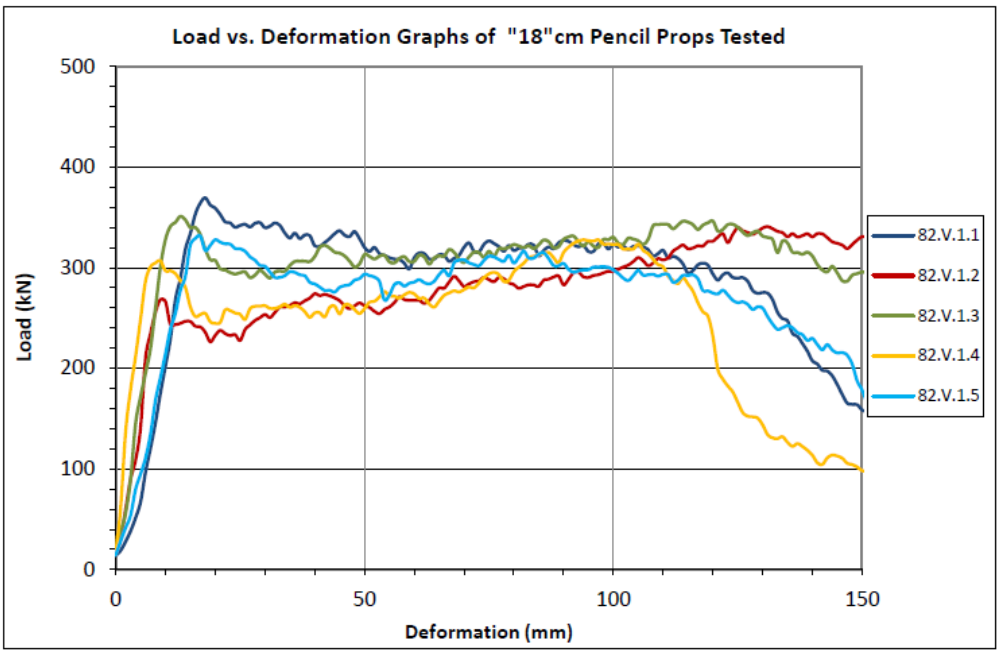

Figure 4.20: Load-deformation chart of 18 cm pencil sticks, 140 mm length (Mabitsela, 2023).

4.6 Pencil Stick Monitoring

Pencil sticks were installed with C-packs as the breaker line during testing. Observations were conducted on the pencil stick effectiveness at a workplace adjacent to the strike stability regional pillar, N15LN02 Panel 001E. The panel length was measured as 30 m (Figure 4.21).

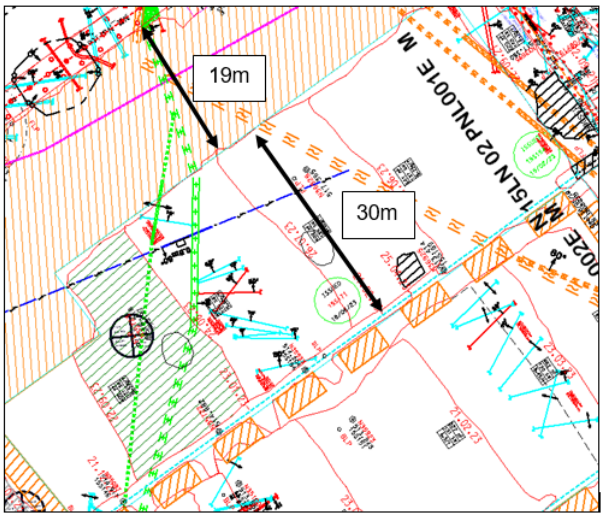

Figure 4.21: N15LN02 Panel 001E layout on Microstation.

The pencil sticks were brushing rapidly after 20 m of installation. Concerns were raised about the long-term stability still being at risk (Figure 4.22). Additional C-packs were installed in all panels where early closure was observed by reducing the strike spacing of the support. Additional visits were introduced to increase monitoring of the panels.



Figure 4.22: Pencil sticks showing rapid yielding.

4.7 Short Panel Observations

The early pencil stick failure meant that additional measures would be required to compensate for the high closure rate. A panel mined at N15LN01 Panel 006W was mined with a 23 m face length from pillar to pillar (Figure 4.23).

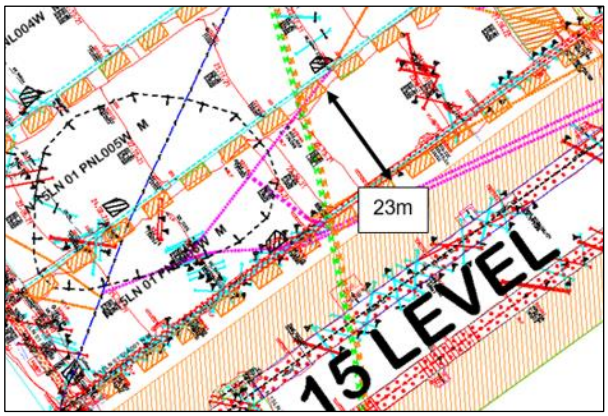

Figure 4.23: Panel 006W layout on Microstation.

The panel was last mined in June 2022, and the condition of the support was fair 12 months after mining was completed to the panel limit. The panel was not redeveloped during its mining cycle and reached the 120 m limit. The support consisted of normal mine poles which had approximately 50% failure in the back areas and approximately 20% failure in the last 30 m to the face. The breaker lines within the last 30 m were intact (Figure 4.24). No signs of falls of ground were observed.



Figure 4.24: Mine pole support in short panel.

4.8 Footwall Heave Hypothesis

The high closure rate was initially considered to be tensile failure of the hangingwall. The data collected from borehole camera, GPR scans and visual observations footwall fractures around the in-stope pillars combined with the tensile cracks observed on the panel footwall are indicators of potential footwall heave. The footwall material is weaker than the hangingwall.

The presence of layers in the footwall with low cohesion, induces foundation instability and pillar punching with heave in the adjacent panels and stope closure (Jager & Ryder, 1999).

Discussions were held with the Geology Department with regards to the Footwall 4 shear. Recent exposures of the footwall 4 shear at a neighbouring mechanised mine led to instability of pillars due to the sheared footwall contact. Exploration drilling data was obtained from the Geology Department for the contact. The data is presented in Table 4.2 below. The average Footwall 4 elevation was located at 4.65 m below the reef. The potential for the contact to form a parting plane is high due to its 1 – 2 cm thick slickensided and serpentinized contact.

Table 4.2: FW4 shear depth from exploration drilling (Shaft Geology Department).

Drillhole No	MR elevation	FW4 shear elevation	Middling (m)
SD254	581.64	587.515	5.875
SD267	560.94	567.33	6.39
SD256	570.17	574.19	4.02
SD270	599.64	602.73	3.09
SD261	592.64	598.42	5.78
SD260	611.28	613.69	2.41
BOS933	574.88	579.87	4.99
BOS880	549.13	553.8	4.67
		Average:	4.65

5 CONCLUSIONS AND RECOMMENDATIONS

5.1 Introduction

In this research report the Hybrid Section stope closure rate was measured. The closure does not appear to be linked to a detachment of a hangingwall parting. The GPR scans and borehole data correlate with the observations made that the hangingwall is stable when not affected by low angled geological structures. The falls of ground that were analysed are structure related and occur in the back areas of the panel after the elongate support had failed due to high closure. Panels with no prominent structures remained stable after the support failure due to the in-stope crush pillars.

5.2 Research Observations

A change of support to pencil sticks was not sufficient to completely cater for the high closure observed despite their relatively high yielding capability. The closure rates were measured to be approximately 1.7 mm/m advance. The pencil sticks would allow for approximately 88 m of advance before their yield capacity would be depleted. The panel length was established as important factor in maintaining stability of the workplaces. Reducing the panel length, allowed a panel to be mined to completion without any structural failures and with reduced support failure.

The combination of reduced closure within the shorter panel length and the increased yield capability of the pencil sticks would provide adequate support for the high closure rates observed.

The pillar footwall material is weaker than the hangingwall and the pillar punches into the footwall (Figure 5.1).

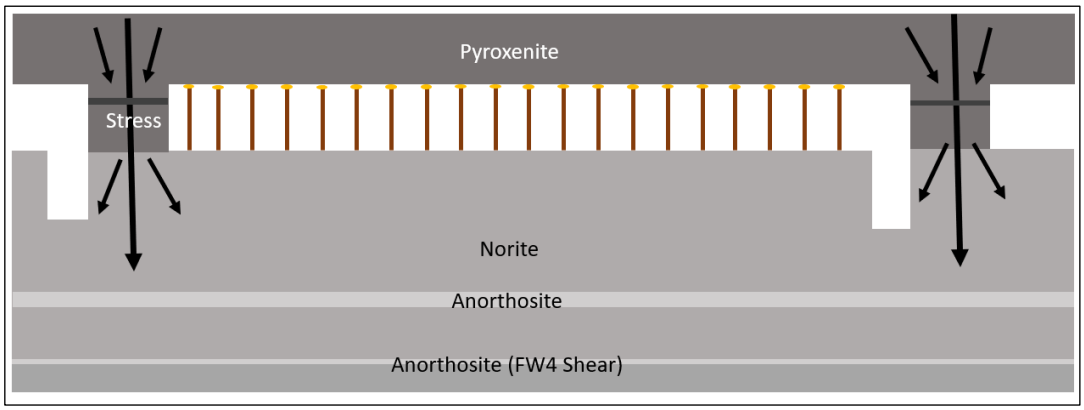

Figure 5.1: Illustration of stress transfer into footwall.

The footwall fractures and tensile cracks in the panel footwall indicate that the stresses are forced to move horizontally due to the Footwall 4 parting plane. The footwall thrusts into the panel causing the elongate failure and high closure rate observed (Figure 5.2).

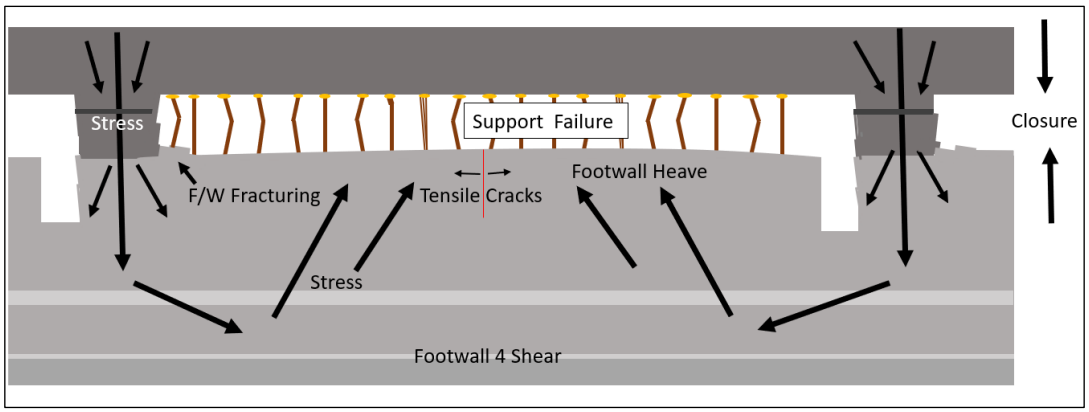

Figure 5.2: Illustration of footwall failure and heave into the panel.

5.3 Research Limitations

The following limitations were found during the research conducted:

- Cover drilling was required for the borehole camera. The location and number of holes were limited due to the size of the equipment being utilised and a tight cover drilling schedule; and
- Damage to closure loggers caused a reduction in closure data available.

5.4 Recommendations

The following recommendations are made based on the research conducted:

- Pencil stick support to be continued as the primary support;
- Panel length to be reduced to 25 m for all new panel layouts; and
- Remaining 30 m panels to be mined with C-Packs installed as back area support.

5.5 Recommendations For Future Research Work

- Load cells installed on the elongates in the new 25 m panels to measure the actual support performance;
- Extensometers to be installed to determine if there is any bed separation at higher levels in the hangingwall;
- Comparison of RMR and Q values in panels where FOG's take place;
- GPR scans of crush pillars with borehole camera correlation to check pillar behaviour; and
- Conduct a study aimed at limiting the mining span between raise lines.

6 REFERENCE LIST

Andrews, P. G., Rwodzi, L., Ekkerd, J. & Ratshitaka, N., 2019. *Advanced techniques for the monitoring of pillar and excavation behaviour at a deep level massive mine: Deep Mining 2019.* Johannesburg, The South African Institute of Mining and Metallurgy.

Bieniawski, Z. T., 1992. *Principles of engineering design for rock mechanics.* Rotterdam, 33rd US Symposium on Rock Mechanics.

Daehnke, A., 2001. Addressing the variability of elongate support performance. *The Journal of The South African Institute of Mining and Metallurgy,* 101(2), pp. 83-90.

Daehnke, A., van Zyl, M. & Roberts, M., 2001. Review and application of stope support design criteria. *The Journal of The South African Institute of Mining and Metallurgy,* 101(3), pp. 135-164.

Dunn, M. J., 2013. *Uncertainty in ground support design and implemetation in underground mining. Ground Support 2013: Proceedings of the Seventh International Symposium on Ground Support in Mining and Underground Construction.* Perth, Australian Centre for Geomechanics.

Jager, A. J. & Ryder, J. A., 1999. *A handbook on rock engineering practice for tabular hard rock mines.* Johannesburg: The Safety in Mines Research Advisory Committee (SIMRAC).

Jones, E. & Beck, D., 2017. *The use of three-dimensional laser scanning for deformation monitoring in underground mines: 13th AusIMM Underground Operators' Conference.* Sydney, AusIMM.

Khosa, B., 2021. *Laboratory Testing Report - 75 x 35 - 10cm C-Pack with Mine Pole - BRPM,* Johannesburg: Groundwork Geotechnical Sensing and Consulting.

Khosa, B., 2022. *Laboratory Testing Report - 140 x 18-20cm Mine Poles - BRPM,* Johannesburg: Groundwork Geotechnical Sensing and Consulting.

Le Bron, K., 2015a. *Rock Engineering Analysis of 4m vent holing at BRPM North Shaft 3rd Phase,* Durban: MLB Consulting.

Le Bron, K., 2015b. *Rock Engineering Back Analysis of K-Value at BRPM North Shaft 3rd Phase,* Durban: MLB Consulting.

Lougher, D. R. & Ozbay, M. U., 1995. In-situ measurements of pillar and rockmass behaviour in a moderately deep hard-rock mine. *The Journal of the South African Institute of Mining and Metallurgy,* 74(1), pp. 246 - 249.

Mabitsela, W., 2023. *Laboratory Testing Report - 140 x 18 - 20cm Pencil Props - Rustenburg Section, Sibanye Platinum,* Johannesburg: Groundwork Geotechnical Sensing and Consulting.

Malan, D. F., 2003. *Guidelines for measuring and analysing continuous stope closure behaviour in deep tabular excavations,* Johannesburg: The Safety in Mines Research Advisory Committee (SIMRAC).

Malan, D. F., 2007. *Monitoring of hangingwall stability at BRPM North Shaft,* s.l.: Unpublished internal company document.

Malan, D. F. & Napier, J. A. L., 2011. The design of stable pillars in the Bushveld Complex mines: a problem solved?. *The Journal of The Southern African Institute of Mining and Metallurgy,* Volume 111, pp. 821 - 836.

Malan, D. F. & Napier, J. A. L., 2021. A review of the role of underground measurements in the historical development of rock engineering in South Africa. *The Journal of the Southern African Institute of Mining and Metallurgy,* Volume 121, pp. 201 - 216.

Malan, D. F., Napier, J. A. L. & Janse van Rensburg, A. L., 2007. Stope deformation measurements as a diagnostic measure of rock behaviour: a

decade of research. *The Journal of The South African Institute of Mining and Metallurgy,* Volume 107, pp. 743-765.

Ozbay, M. U., Ryder, J. A. & Jager, A. J., 1995. The design of pillar systems as practiced in shallow hard-rock tabular mines in South Africa. *The Journal of The South African Institute of Mining and Metallurgy,* 95(1), pp. 7 - 18.

Pienaar, A., 2017. *The Sub Surface Profiler: a giant leap for ground penetrating radar.* Stellenbosch, Reutech Mining.

Piper, P. S., Malan, D. F., Clements, T. N. & Janse van Rensburg, A. L., 2007. *The real in-situ performance of pre-stressed elongates.* Free State, SANIRE Symposium - Redefining the boundaries II, pp. 15-34.

Roberts, D. P., Roberts, M. K. C., Jager, A. J. & Coetzer, S., 2005. The determination of the residual strength of hard rock crush pillars with a width-to-height ratio of 2:1. *The Journal of The South African Institute of Mining and Metallurgy,* Volume 105, pp. 401 - 408.

Stacey, T. R., 2009. Design - a strategic issue. *The Southern African Institute of Mining and Metallurgy,* Volume 109, pp. 157 - 162.

Swart, A. H., 2005. *Investigation of factors governing the stability of stope panels in hard rock mines in order to define a suitable design methodology for shallow mining operations. MSC Engineering (Mining),* Pretoria: University of Pretoria.

Swart, A. H. & Handley, M. F., 2004. *The design of stable stope panels for near-surface and shallow mining operations. International Platinum Conference ' Platinum Adding Value'.* s.l., The South African Institute of Mining and Metallurgy.

Watson, B. P., 2004. A rock mass rating system for evaluating stope stability on the Bushveld Platinum mines. *The Journal of The South African Institute of Mining and Metallurgy,* 104(4), pp. 229 - 238.

Watson, B. P., Kuijpers, J. S. & Stacey, T. R., 2010. Design of Merensky Reef crush pillars. *The Journal of The Southern African Institute of Mining and Metallurgy,* Volume 110, pp. 581 - 591.

York, G., Canbulat, I., Kabeya, K. K., Le Bron, K., Watson, B. P. &Williams, S. B., 1998. *Develop guidelines for the design of pillar systens for shallow and intermediate depth, tabular, hard rock mines and provide a methodology for assessing hangingwall stability and support requirements for the panels between pillars. SIMRAC Report GAP 334,* Pretoria: CSIR Mining Technology.